CIRM 11
March 1998

NATIONAL PHYSICAL LABORATORY

Measurements of the response functions of PADC track-etch and NTA film personal neutron dosemeters over the energy range from 100 keV to 5 MeV

by

D. W. Drew and D. J. Thomas

Centre for Ionising Radiation Metrology

Abstract.
This report describes an extensive set of measurements of the response functions of PADC track-etch and NTA film personal dosemeters from UK Approved Dosimetry Services. A novel technique for producing simultaneous irradiations over a range of neutron energies is employed to provide detailed results for response characteristics over the energy range from about 100 keV to 1.2 MeV. Two further measurements have been performed at 2.5 and 5.0 MeV to extend the data to higher energies. The report presents the results for both the fluence and personal dose equivalent response functions, and discusses these results and their implications.
Note: all uncertainties quoted in this report are estimates of standard (1σ) uncertainties representing a confidence level of approximately 67%.

ISSN 1369-6793

National Physical Laboratory
Teddington, Middlesex, UK, TW11 0LW

Approved on behalf of Managing Director NPL, by Dr Julian Hunt
Director, Centre for Ionising Radiation Metrology.

CONTENTS

1. INTRODUCTION

At present, in the UK, and in most other countries, control of the occupational exposure of classified radiation workers is realized by estimating and limiting the effective dose equivalent received from radiation of all types. For external radiation, the estimates of this quantity are normally derived from the reading of personal dosemeters worn by the individual.

Effective dose equivalent as defined by the International Commission on Radiological Protection (ICRP), is a weighted mean of dose equivalents in various organs of an anthropomorphic phantom representing the human body, and is therefore usually considered as a quantity which cannot be measured directly by any practical device. In view of this, so called operational quantities were introduced by the International Commission on Radiation Units and Measurements (ICRU) for both area survey measurements and personal monitoring[1]. These were designed to be measurable and to be conservative estimates of the quantity effective dose equivalent.

For personal monitoring, the operational quantity is personal dose equivalent, $H_p(d)$, which is defined (see for example reference 2) as the dose equivalent in four-element soft tissue (mass composition: 76.2% oxygen, 11.1% carbon, 10.1% hydrogen, and 2.6% nitrogen) at a depth d below a specified point on the body. The specified point is usually taken to mean the point where a dosemeter is worn. The depth, d, depends on the penetrating power of the radiation, but for neutrons of all energies, d has the value of 10 mm. Metrologically this is a somewhat inexact definition since details of the body are not specified, and for this reason, for the performance of calibrations, a calibration quantity is defined, see reference 3. This is $H_p(d)$ in a theoretical phantom having the composition of ICRU tissue, and the same shape and size as the actual calibration phantom.

Practical considerations and common usage have narrowed the choice of calibration phantom for whole body irradiation down to a block measuring 30 x 30 x 15 cm. Fluence to personal dose equivalent conversion coefficients have been calculated for an ICRU tissue phantom of this size as a function of energy so that the value of $H_p(d)$ can be derived for any neutron field incident on the phantom from a knowledge of the neutron fluence and the spectrum.

No material with the composition of ICRU tissue exists from which a calibration phantom could be constructed, and different tissue substitute materials, such as polymethyl methacrylate (PMMA) or water, have tended to be used. The recommendation of the International Organization for Standardisation (ISO) is that no corrections should be made for differences between the compositions of the actual and calculational phantoms provided calibrations are performed with a particular type of water phantom whose design has been specified by ISO [4].

A quantity has thus been defined, which personal dosemeters should be designed to measure. One of the fundamental problems of neutron dosimetry is, however, that it has, to date, proved impossible to design a personal dosemeter which has the required response characteristics over the full range of energies encountered in radiation protection. There is thus the potential for presently available neutron personal dosemeters to significant under- or over-estimate the operational quantity, and this undermines confidence in their results.

In the UK, the majority of neutron dosemeters issued by approved dosimetry services use either the plastic PADC (poly-allyl diglycol carbonate, often known by the trade name CR-39) or NTA film as the sensor element.

PADC is a material which can be used to detect charged particles, provided the energy deposited by these particles is sufficiently intense and localised. The damage tracks formed by these particles can be etched to form pits and the number of these pits can be counted. PADC's ability to detect the recoil protons produced by neutrons in a hydrogenous layer enables it to respond to fast neutrons, and its response function for these fast neutrons approximately satisfies the requirements for measuring the quantity personal dose equivalent above an energy threshold which normally lies in the 100 to 200 keV region. For neutrons below the threshold energy the personal dose equivalent response is almost negligibly small, and the presence of a sizeable dose equivalent in the low-energy region presents the potential for significant under-reading by the dosemeter. To mitigate against this, some services include in their PADC-based dosemeters a material which gives it a thermal neutron sensitivity. An example of this would be a piece of nylon in close proximity to the sensor. Thermal neutrons undergo capture by the nitrogen in the nylon producing protons of about 600 keV which can be detected in the PADC. This gives the device some of the characteristics of an albedo dosemeter, i.e. one which detects thermal and epi-thermal neutrons backscattered from the wearer. By careful design the dosemeter can provide a personal dose equivalent response at thermal energies and also over some of the epi-thermal region. There still remains, however, an energy region, below the fast neutron threshold, where the dosemeter seriously underestimates personal dose equivalent.

NTA film has neutron energy response characteristics with features which exhibit certain similarities to PADC in terms of the overall shape. Again there is a threshold below which the dose equivalent response is negligibly small. However, this occurs at a higher neutron energy, somewhere between 500 and 600 keV, so the potential for missing part of the dose equivalent is greater. The NTA film is inherently sensitive to thermal neutrons, due to the presence of nitrogen in the film. Designing the dosemeter to give the correct thermal response, however, presents complications and involves the use of just the right amount of a thermal neutron absorbing material, e.g. ^{10}B, to reduce the thermal response to the required level. Because of this, it is not uncommon for designers of dosemeters based on NTA film to completely remove any thermal sensitivity by including a sufficiently thick layer of a good neutron absorbing material, such as cadmium, to absorb all the thermal neutrons, leaving the dosemeter as a purely fast-neutron measuring device.

To estimate the extent of any misreading by a personal dosemeter in a working environment two items of information are essential:

(i) the neutron spectrum of the field in which the dosemeter is used,
(ii) the dosemeter response function over the energy range where neutrons are present.

In addition to the energy information, it is also important to have data on the angular dependence of both the field and the dosemeter response characteristics if a detailed estimate of the personal dose equivalent is to be made. Knowing the energy characteristics, however, allows the 'worst case' situation to be quantified.

In the majority of situations, workplace spectra are not known. However, there now exists a data base of measured and calculated spectra, with a dedicated data handling program[5], which can be used, if a dosemeter's response function is known, to determine that dosemeter's likely under- or over-readings in a variety of environments. Use of this facility can provide information on potentially hazardous situations where dosemeters could under-respond significantly.

Personal dosemeter response functions tend to only be measured approximately, mainly due to the time and expense needed to measure the full response function in detail. This needs to be done with monoenergetic neutrons, and, up until now, has always involved a very extensive experimental programme because each energy requires a separate measurement. Typically response functions are based on about six monoenergetic measurements, and errors can occur in regions where the data have to be interpolated.

Recent developments at NPL have, however, provided a more efficient procedure for determining the response function over the important energy range around, and just above, the threshold energies for PADC track-etch and NTA film dosemeters. This region is particularly important because the dose equivalent response varies rapidly with energy. A facility, described in detail in reference 6, allows simultaneous irradiations to be performed for a set of dosemeters over a range of known energies.

Neutrons covering a large part of the energy range from about 1 keV to 20 MeV can be produced using various nuclear reactions and different bombarding particles from the NPL 3.5 MV Van de Graaff accelerator. The normal procedure for performing irradiations involves setting up the facility to produce a particular neutron energy, standardizing the fluence at this energy, and making measurements solely at that one energy. This is a very time consuming approach.

For a number of the neutron-producing reactions, ^{7}Li(p,n)^{7}Be and T(p,n)^{3}He being good examples, the energy of the neutrons varies significantly with angle of emission relative to the direction of the bombarding charged particle beam. This is a simple consequence of the reaction kinematics, and the energy can be calculated directly using the laws of momentum and energy conservation. This means that, for physically small devices such as personal dosemeters, it is possible, by arranging them in an arc at different angles relative to the charged particle beam, to provide simultaneous irradiations of a number of dosemeters over a range of neutron energies.

Although the energies as a function of angle can easily be calculated from the kinematics, the same is not true for the fluence. Tabulated angular distribution data for these reactions are available[7,8] but the accuracy is not specified. For this reason three dedicated irradiation fields have been characterised by selecting a particular target and set of bombarding conditions, and carefully measuring the variation of the neutron fluence with angle for neutron emission angles from 0° to 75° on either side of the direction of the bombarding charged particle beam. These data enable the fluence at any angle to be derived from that measured at 0° using the normal standardisation procedures.

The three irradiation fields characterised in this way were:

Field A: 101 keV (75°) to 250 keV (0°) derived from the ^{7}Li(p,n)^{7}Be reaction using a proton bombarding energy of 2019 keV,

Field B: 336 keV (75°) to 565 keV (0°) derived from the ^{7}Li(p,n)^{7}Be reaction using a proton bombarding energy of 2296 keV,

Field C: 561 keV (75°) to 1200 keV (0°) derived from the T(p,n)^{3}He reaction using a proton bombarding energy of 2017 keV.

The readings of single personal dosemeters tend to exhibit uncertainties, which, even for the optimum dose in terms of reading tracks or pits on the sensor elements, are never less than about

10%. For this reason a number are usually irradiated simultaneously during a response function measurement in order to reduce this uncertainty. Due to the symmetry of the irradiation about the proton beam direction for the multi-energy irradiation fields described above, the energies are the same at corresponding angles on either side of 0°. Thus, except for the energy corresponding to 0°, at leat two dosemeters are irradiated at each energy. For physically small dosemeters more than one can be mounted at each angle, thus further increasing the number irradiated. Also, because the facility provides results at closely spaced energies, the correlations which exist between adjacent energies, in that the responses cannot differ very greatly between adjacent energies, and the fact that this variation should be smooth, all help to reduce the overall statistical uncertainty in the derived response function.

The aim of the present work was to measure response function data for a number of PADC track-etch and NTA film dosemeters. The multi-energy irradiation fields provide data over the energy range from about 100 keV to 1.2 MeV. However, there is a need to extend the data to energies above this range. Above the threshold region the response function is not expected to vary very significantly with neutron energy, and so only two additional monoenergetic point values were considered necessary. Measurements were performed at 2.5 MeV and 5.0 MeV using the conventional irradiation techniques for monoenergetic neutrons. The 2.5 MeV neutrons were produced using the $T(p,n)^3He$ reaction, whilst those at 5.0 MeV were produced with the $D(d,n)^3He$ reaction. Except for areas around high-energy accelerators, and environments where cosmic rays are significant, the neutron spectra in environments where classified workers are exposed rarely extend above 5 MeV.

Although all dosemeters which use PADC as the sensor element detect neutrons in essentially the same way, differences arise in their response function shapes due to differences in parameters such as: the characteristics of the plastic, the etching technique, the design of the holder for the PADC, and the way in which the damage pits are counted. Similarly, differences can also occur between service providers using NTA film. In order to try to quantify these differences, with a view to subsequently investigating their implications for dosemeter performance in various typical fields, measurements were made for all dosimetry services which have been approved by the Health and Safety Executive (HSE) in the UK, and which were operational at the time of the measurements. For PADC sensors there were three services, and one of these offered two types of PADC dosemeter. Measurements were performed over the range 101 keV to 5 MeV for the four types of PADC dosemeters, and they have been identified in this document by the codes P1 to P4. For NTA film there were two services offering this type of dosemeters, although they were very similar in design. Measurements for these extended over the energy range 561 keV to 5 MeV, and they have been identified as N1 and N2.

This report presents the results of measurements of dosemeter response functions above about 100 keV, and it is planned to subsequently use this information to investigate personal dosemeter performance in realistic fields. For this work additional data on the thermal and epi-thermal response will be needed for those dosemeters with a thermal sensitivity. Dose equivalents in the low-energy region are usually less significant than those at higher energies and the data for responses in the low-energy region, where needed, can be obtained from earlier measurements performed by the dosimetry services.

2. THE EXPERIMENTS

Neutron fields for the response function measurements described here were produced using one of three nuclear reactions, either $^{7}Li(p,n)^{7}Be$, $T(p,n)^{3}He$, or $D(d,n)^{3}He$, with the proton or deuteron charged particle beams being generated by the NPL 3.5 MV Van de Graaff accelerator.

Neutrons of the desired energy were produced by selecting the appropriate reaction and the correct charged particle bombarding energy. An energy selection magnet, with an NMR feedback control, allows bombarding energies to be set to within an uncertainty of about ±3 keV. Neutron energies, and energy resolution values, are calculated from the reaction kinematics, and the known energy loss of the charged particle beam in the neutron-producing target layer.

The neutron fluence rate depends on the reaction cross section and the beam current. Restrictions on the allowable beam currents arise because of target heating. To minimise this heating the charged particle beam is de-focussed to an area of 3 to 4 mm diameter, and this in turn is modulated by applying an electric field to scan the beam into a circle to create a diffuse beam 'spot' of about 10 mm diameter. Despite this, and air cooling of the target, temperature rises occur which can result in loss of material from the target layer if the beam current is too high. This limits the maximum neutron yield attainable, and resulted for the present measurements in irradiation times which typically needed to be several hours duration to obtain optimum dose equivalent values for irradiating the dosemeters.

The fluence rates were measured using the NPL standard long counter. This instrument has been thoroughly characterised and its efficiency determined as a function of neutron energy(9). The procedure for determining the fluence delivered during the irradiation of the dosemeters involves several stages. These are explained in reference 6, but are outlined here for completeness.

Firstly the long counter is positioned at 0° to the charged particle beam direction, at a distance of between 1.5 and 2.0 m from the target, and a measurement is made of the total incident fluence relative to the readings of two monitors. The first of these monitors is the beam current, as measured with a current integrator, and the second is a high-efficiency moderating detector mounted permanently on the laboratory wall. A measurement is then made with a shadow cone positioned to eliminate all neutrons arriving at the long counter directly from the target so that its response to scattered neutrons originating from all parts of the room is measured. These two measurements provide a calibration of the two monitors in terms of the direct fluence (neutrons per cm^{2}), at 0°, per monitor count. The long counter is then positioned as far from the target as possible, to minimise scatter from this device, and the irradiation of the dosemeters is performed with the fluence delivered being determined from the monitor readings.

The beam current is used as the primary monitor because it is insensitive to scattering from whatever devices are placed in the neutron field. This is not the case for the moderating detector. A check is, however, always made of the ratio of the two monitor readings to ensure that it does not vary by more than would be expected from changes in the moderating detector readings due to scattering objects in the neutron field.

Since the position and profile of the beam spot on the target layer can vary a little every time an experiment is set up, and the target layer is not completely uniform, the calibration of the monitors has to be performed every time the Van de Graaff accelerator is started up, and also every time the beam energy is changed.

All the irradiations were performed in the NPL low-scatter neutron laboratory. This is a large shielded room with a length of 25 m and a width of 18 m. The neutron producing targets are positioned above the centre of an approximately 12 m diameter circular pit situated at one end of the room so that the nearest solid scattering surface is a distance of 6 m from the target position.

A detector transport system, consisting of four arms, each of which incorporates a movable trolley is available for mounting devices which are to be irradiated. These were utilized for mounting the long counter and for the phantom used in the monoenergetic measurements. The four arms are pivoted about the centre of the pit so that devices can be positioned at any angle relative to the direction of the bombarding charged particle beam. The trolley on each arm can also be moved along the arm to obtain any required device to neutron-producing target distance between a few cm and about 5 m.

For the present measurements, both those with the multi-energy fields and those with monoenergetic neutrons of 2.5 and 5.0 MeV, all the dosemeters were positioned at a nominal distance of 75 cm from the beam spot on the neutron-producing target. This is the distance recommended by ISO(10) and is a compromise between various conflicting requirements.

In order to ensure an even distribution of fluence over several dosemeters arranged on the surface of a slab phantom, particularly when the neutron distribution is non-isotropic, the neutron source to dosemeter distance needs to be maximised. Increasing the distance also reduces uncertainties introduced by the fact that the source is not actually a point. Another reason for using a reasonably large distance is that it reduces the percentage uncertainty in measuring the distance. This needs to be known accurately since it is used to determine the fluence at the dosemeter, and the fluence has an inverse square law dependence on the distance. The uncertainties in the distance, which are of the order of 1 to 2 mm, occur, for example, because of uncertainty in determining the exact position of the target layer. They are largely independent of the overall distance up to about 2 m, and so the percentage effect decreases as the irradiation distance increases.

However, there are also arguments for keeping the neutron source to dosemeter distance short. Firstly, personal dosemeters are not particularly efficient devices, and hence reducing the irradiation distance increases the fluence and reduces the required irradiation times. These nevertheless still amount to several hours. The second reason for reducing the distance arises from the effects of scattered neutrons. The dosemeters are subjected not only to direct neutron bombardment from the neutron producing target, but also to neutrons which are scattered towards the dosemeters from the walls, floor, and ceiling of the experimental area, and also by the air and equipment within the room. These are of different energies to the primary neutrons, their numbers are not usually known, and their effects are thus difficult to determine. The air and equipment scattered component varies roughly as the inverse of the source to dosemeter distance, whilst the room component is roughly constant. Since the direct component has an inverse square dependence on the distance, reducing the distance decreases the percentage contribution from scattering. In the large low-scatter area in which the measurements were performed, evidence from other work(11) indicates that the scattered neutron contribution to the dosemeter response is essentially negligible at 75 cm. No correction is therefore applied for this effect, although a small additional uncertainty component is included in the final uncertainty. One factor which helps in this matter is that the scattered component has a reasonably isotropic incidence on the dosemeters and the efficiency of both PADC track-etch and NTA film dosemeters is a maximum for normal incidence, i.e. for the neutrons arriving directly from the target, and decreases as the angle of incidence relative to the dosemeter face decreases. Also, there is some element of cancellation because the response to in-scattered neutrons is partly compensated by the loss of some of the direct component by out-scatter in the air between the neutron source and the long counter.

2.1 Measurements using the multi-energy irradiation fields

Detailed descriptions of the energies and angular distributions of the three multi-energy irradiation fields, A, B, and C, used for this work are given in NPL Report CIRM 10[6]. Each field allows dosemeters to be irradiated at a number of known energies depending on the angle at which the dosemeter is placed relative to the direction of the charged particle beam.

The dosemeters were mounted on a support ring arrangement to ensure that they were all positioned at a nominal distance of 75 cm from the beam spot on the neutron-producing target. This ring is made of aluminium, and is very lightweight. Although it is 3 cm wide and 1 cm thick, numerous holes in the metal reduce the overall mass. The ring is supported on thin hollow aluminium tubes which radiate upwards and outwards from a small ring which fits over a boss at the centre of the pit. In this way the centre of the support ring is positioned just below the neutron-producing target.

Dosemeters are mounted on posts set into the ring at regular intervals. This allows the dosemeters to be positioned in a horizontal plane at the height of the charged particle beam, and at any angle relative to the beam. By convention angles to the left of the beam direction are designated as negative angles and those to the right as positive. The upper part of each post is made up of a flat rectangular piece of aluminium (63 mm long, by 13 mm wide and 1.6 mm thick) set with its long side vertical and with a flat side facing the source of neutrons. A rectangular hole in the flat face further reduces the amount of material present. Dosemeters were attached to the flat face using either double-sided adhesive tape, or the dosemeter's own clip if appropriate.

An optical surveyor's level, positioned at the edge of the pit and on the 0° line, was used to align the ring in the horizontal plane. When more than one dosemeter was attached to each aluminium flat the height of each dosemeter above or below the horizontal plane of the charged particle beam was measured in order to derive distance corrections for use when calculating the incident fluence on each dosemeter. Due to a slight asymmetry in the ring arrangement, there is a variation in the irradiation distance of roughly 5 mm around the ring, and consequently it was necessary to measure the distance for each angle.

The optimum dose equivalent value for reading PADC track-etch dosemeters is in the region of 3 to 5 mSv. For NTA film it is somewhat higher, possibly up to 10 mSv. Dose equivalent rates from the three Fields A, B, anc C, are low, and they vary significantly with the angle, and hence with the neutron energy, being a maximum at 0° and a minimum at 75°. It is thus difficult to deliver the optimum dose equivalents to all dosemeters, and in some cases it is difficult to deliver the optimum dose equivalent, even for the maximum rate, within a reasonable timescale.

For Field A, the energy varies from 101 keV at 75° to 250 keV at 0°. The maximum personal dose equivalent rate which can be delivered at 0° is about 0.62 mSv h^{-1}, and this decreases to about 37% of this value at 101 keV. Irradiations in Field A were only performed for the PADC track-etch dosemeters and took up to seven hours, delivering in this time dose equivalents of the order of 4.5 mSv at 250 keV and 1.7 mSv at 101 keV. A measurement for a set of dosemeters thus took a whole day, and even then the dose equivalent delivered at 101 keV was lower than the optimum. Enough tracks were , however, produced to make reasonable measurements.

For Field B, where the neutron energies vary from 336 keV at 75° to 565 keV at 0°, the dose equivalent rates are higher, being about 2.6 mSv h^{-1} at 565 keV. The decrease in rate with angle is more rapid than for Field A, and the rate at 336 keV is only 22% of that at 0°. Reasonable dose equivalent values at 0° could thus be obtained in two to three hours. However, because of the larger variation of dose equivalent with angle for this field, the dosemeters over the angular range from 0° to 50° were removed, after a reasonable dose equivalent had been accumulated, and the irradiations were continued to increase the dose equivalent delivered to the dosemeters at angles between 55° and 75° to at least 2 mSv. Due to the higher dose equivalent rates it was possible to measure two sets of dosemeters in a single day. Again this field was only used for the PADC track-etch dosemeters since NTA film was not expected to have a measurable response over this energy range.

For Field C, the neutron energy ranges from 561 keV at 75° to 1200 keV at 0°, with maximum achievable dose equivalent rates of about 0.45 and 0.18 mSv h^{-1} respectively. As for Field A, whole day irradiations were required to obtain reasonable overall dose equivalent values. For the irradiations of both types of dosemeter the dose equivalent values were roughly 3.5 mSv at 1200 keV and 1.4 mSv at 561 keV. For NTA film in particular, these are not ideal, and larger values would have been preferable, but they were nevertheless adequate, and gave reasonable track densities on the NTA film.

Monoenergetic measurements

Measurements using monoenergetic neutrons were performed at 2.5 and 5.0 MeV. The 2.5 MeV neutrons were produced using the $T(p,n)^3He$ reaction where the maximum attainable 0° personal dose equivalent rate was about 1 mSv h^{-1}. Neutrons at 5.0 MeV were produced using the $D(d,n)^3He$ reaction and here the maximum attainable 0° dose equivalent rate was about 2 mSv h^{-1}. At both these energies it was thus possible to irradiate several sets of dosemeters in a single day.

The measurements with monoenergetic neutrons were performed with the dosemeters mounted on the front face of a 30 x 30 x 15 cm ISO slab phantom positioned at 0° to the charged particle beam and with the front face positioned at 75 cm from the neutron producing target. The ISO slab phantom(4), commonly referred to as a water phantom, is a container, constructed with PMMA plastic walls, which is filled with water. All the walls are 10 mm thick, except for that forming the front face which is 2.5 mm thick. Dosemeters were attached using double sided adhesive tape, and were positioned within a 20 x 20 cm square at the centre of the front face to avoid edge effects(12). Corrections were performed for the reduced fluence for dosemeters displaced from the centre resulting from the slightly increased neutron source to dosemeter distance. Further small corrections were also made for the reduction in the fluence and the energy for angles other than 0°. These were derived from the tabulated data of Liskien and Paulsen(7).

Phantom backscatter effects

Phantoms are important concepts in the measurement of personal dose equivalent; their presence being implicit in the definition of the quantity. They also serve the function of providing backscattered radiation during a calibration. When worn by individuals personal dosemeters are subjected to both direct radiation and radiation backscattered from the human body. This latter component can be very important, and is the basis of the response of neutron albedo dosemeters which predominantly measure backscattered thermal and epi-thermal neutrons from the body. In the calibration situation the phantom plays the role of the body in providing this backscattered radiation.

PADC track-etch and NTA film sensors are, however, predominantly fast neutron detecting devices. Both can also respond, either directly or indirectly, to thermal and epithermal neutrons, but in the normal calibration situation, which involves the use of fast neutrons, usually from an ^{241}Am-Be or a ^{252}Cf neutron source, the reading of the sensors is dominated by events caused by the incident direct neutrons. A recent experimental and calculational investigation of the backscatter from calibration phantoms[12] showed that, for the ISO water phantom, for both ^{241}Am-Be and ^{252}Cf neutrons, for either PADC track-etch or NTA film dosemeters, the contribution to the reading from backscatter is small, being typically about 5%. A calibration phantom can thus be dispensed with in situations where its presence would make the measurements particularly difficult or impractical, and corrections can be applied for the missing backscatter.

The present measurements with the multi-energy irradiation fields is an example of a case where a phantom would be impractical. Dosemeters are distributed over an arc from -75° to 75° about the direction of the charged particle beam which produces the neutrons, and a phantom covering this arc would provide entirely inappropriate scattering into the detectors.

Backscattered neutrons from a phantom are of lower energy than the incident neutrons, and many thus fall below the energy threshold in the PADC track-etch and NTA film dosemeter response. This effect is one of the reasons why their response to backscatter is small. The energies of the neutrons used in the multi-energy irradiations are even lower than those used in the measurements of backscatter response, and thus the backscatter reading would be expected to be even lower than the value of 5% determined for ^{241}Am-Be and ^{252}Cf neutrons.

For devices with a thermal response the percentage contribution to the dosemeter reading which results from backscattered thermal neutrons increases as the energy decreases; simply because the response to the direct neutrons is falling rapidly. Even at the lowest energies involved, however, the reading due to backscattered thermals from a phantom is still expected to be a small fraction of the reading due to the direct neutrons, and for this reason no corrections for backscatter were made in the multi-energy measurements. In view of the relatively large uncertainty in personal dosemeter measurements the effect would be extremely difficult to measure.

The two monoenergetic measurements were performed at higher energies where backscatter is more significant, and an ISO water phantom was used in all these measurements.

2.4 The reference point of the dosemeters

Guidance presently being formulated by the ISO[4] on calibration of dosemeters uses the concept of a *reference point* associated with each dosemeter. During a calibration this reference point is positioned at the *point of test*, i.e. that point in the radiation field where the conventional true value of the quantity to be measured is known. For a receptor-free quantity, e.g. ambient dose equivalent, which is the operational quantity for area survey instruments, this presents no conceptual difficulties since the quantity is defined at a point. For personal dose equivalent, which is in every respect a receptor-dependent quantity, problems arise from the above calibration prescription.

For neutrons, personal dose equivalent is defined as the dose equivalent at a depth of 10 mm below a specified point on the body, or in the calibration situation, the phantom. Although the quantity is defined in terms of a dose equivalent at this particular depth, this dose equivalent is the result of the neutron fluence incident on the outside of the body, or the phantom. Calculation of the fluence to dose equivalent conversion coefficients to be used in a calibration are performed for a plane parallel beam striking the front face of the phantom. Thus, in the calibration situation, where the fluence usually results from an essentially point source of neutrons, and hence varies as the inverse square of the distance from the source, the fluence used to calculate the dose equivalent must be that at the front face since this provides the best replication of the setup in the calculation of the conversion coefficients. This situation does not, however, easily equate with the ISO concept outlined above, since identification of the exact reference point in this extended phantom-plus-dosemeter assembly is not obvious, and no prescriptive guidance is given by ISO.

If the calibration is simply viewed as a procedure whereby a dosemeter is mounted on the face of a phantom, the personal dose equivalent is calculated from the conversion coefficients and the fluence on the phantom surface, and the dosemeter reading is equated to the calculated dose equivalent, the concepts of point of test and reference point do not need to be invoked. There is, however, then a problem when no phantom is used. A solution to this is to define the reference point as being on the back face of the dosemeter, at the point where it would touch the phantom, if a phantom were being used. This choice of reference point has advantages when the angular dependence of dosemeters is investigated.

The above convention for the reference point was used for all the present measurements, whether "free-in-air" or "on-phantom" with the exception of those for one particular type of PADC track-etch sensor where three layers of PADC plastic elements where used to increase the number of data values at each energy and hence improve the statistical accuracy. The elements in the layer nearest the source were exposed to a slightly higher fluence than the next layer, which in turn saw more fluence than the furthest layer. To correct for this the reference point was taken to be at the rear surface of the sensor element, i.e. the surface away from the direction of the incident neutrons. Ideally the reference point should be some distance behind this rear surface, at the position where the back surface of the dosemeter would be located. Since this distance was not known exactly, because the exact positioning of the sensor element in the dosemeter holder under normal use was not known, the above approach to providing corrections for the slightly different fluences seen by the sensor elements was considered acceptable, particularly since the quantity under investigation is primarily the shape of the response function rather than the absolute magnitude. The three layers of sensors were always treated separately in the analysis, and were kept separate in order to distinguish any differences between the results for the different layers.

3. MEASUREMENT DETAILS AND RESULTS

The main parameter derived from the series of experiments reported here is the fluence response function, i.e. the variation of the track density per unit fluence with neutron energy, for various personal dosemeters. (The fluence response, which is tracks per cm^2 divided by neutrons per cm^2, is sometimes referred to simply as tracks per neutron.) This response is related to a primary field quantity, i.e. neutron fluence, and is hence not dependent on any particular conversion coefficient which may be used to convert from fluence to dose equivalent. These coefficients may change with time.

Nevertheless, dosemeters are usually intended to measure the operational quantity personal dose equivalent, $H_p(d)$. For this reason the personal dose equivalent response function is also presented here for each dosemeter set, and the particular conversion coefficients used are those calculated for 10 mm depth in a 30 x 30 x 15 cm slab of ICRU tissue for normal incidence of the neutron radiation. These coefficients, denoted as $h_{p,slab}(10)$, allow a 'calibration' quantity, $H_{p,slab}(10)$, to be derived, which is taken as an acceptable estimation of the personal dose equivalent. They have been calculated by Hollnagel(13) using the quality factor to lineal energy relationship, Q(L), given originally in ICRP Publication 15(14), and correspond to the operational quantity as realised prior to the recommendations of ICRP Publication 60(15).

Different services read different sized areas on the sensor elements, varying from about 10 mm^2 to over 1 cm^2. The larger the area read, the more tracks recorded, and the smaller the statistical uncertainty; although effects other than statistics tend to ensure that the uncertainty on a single dosemeter reading cannot usually be reduced below about 10%. For the results presented here all the data, however reported, whether as events in a fixed area, or events per cm^2, or event per mm^2, have been converted into events per cm^2 in order to present all the data on the same basis.

3.1 Dosemeter set P1

Dosemeter set P1 included sensor elements from four individual sheets of PADC plastic. Each of the sheets had been produced in the same manner, by the same manufacturer, and were nominally all the same. The four sheets were designated A, B, C, and D respectively. Each dosemeter was labelled with a letter indicating the sheet from which it originated, and an identifying number. There were 62 dosemeters for each of the three multi-energy fields, and 24 for each of the mono-energetic neutron energies, 2.5 MeV and 5.0 MeV, see Table 1. A number of dosemeters from each sheet, adding up to a total of 26 in all, were supplied to act as controls. Data indicating how the dosemeters from the three sheets should be divided between the different irradiation conditions were supplied by the service.

Table 1. Organisation of the dosemeters for the various irradiations

Energies	Sheet A	Sheet B	Sheet C	Sheet D	Total
100 - 250 keV	16	16	15	15	62
336 - 565 keV	15	15	16	16	62
561-1200 keV	16	16	15	15	62
2.5 MeV	6	6	6	6	24
5.0 MeV	6	6	6	6	24
Controls	6	6	7	7	26

For each of the multi-energy fields two dosemeters were placed at each post on the support ring, and the posts were positioned at 5° intervals from -75° through 0° to +75°. The arrangement for mounting the dosemeters at each position upon the support ring involved firstly attaching the two dosemeters to a strip of card with double-sided adhesive tape. An elastic band was then used to hold each card in place on the support post in such a way that one dosemeter was above the horizontal plane defined by the bombarding proton beam, the other below.

The dosemeters of set P1 are rectangular, and the part of the PADC sensor element which is processed for track counting is located towards one end of the rectangle. The dosemeter positioned above the horizontal plane was therefore orientated with this end downwards, while the dosemeter below this plane was orientated in the opposite way so that both processed areas of PADC had the same offset with respect to the height of the source of neutrons. Both dosemeters on a given post were thus irradiated with neutrons of the same energy and fluence. Dosemeters with elements from sheets A and B were attached to the same card, with the dosemeter containing an element from sheet B above the horizontal plane. Likewise, dosemeters with elements from sheets C and D were attached to the same card with the dosemeter containing an element from sheet D above the horizontal plane.

The cards were fixed to the support posts in such a way that those containing elements from sheets A and B alternated with those containing elements from sheets C and D. Further, if dosemeters with elements from sheets A and B were placed at a given angle, dosemeters with elements from sheets C and D were placed at the corresponding angle on the other side of the support ring. This ensured that one element from each sheet was irradiated with neutrons of each energy; the only exception being for the post at 0°. With this arrangement the four sheets of PADC could be checked for variability in their response. Irradiation of the dosemeters followed the procedure outlined in section 2.1

For irradiation with 2.5 and 5.0 MeV monoenergetic neutrons, the dosemeters were attached directly to the phantom with doubled sided adhesive tape. Although the variation of energy and fluence over the surface of the phantom is not large, the distribution over the phantom face of the dosemeters containing elements from the different sheets followed the pattern outlined above, in the sense that they were arranged as symmetrically as possible about the centre of the phantom. In this way, wherever possible, there was a dosemeter with an element from each of the four sheets at a given neutron angle relative to the direction of the bombarding proton beam. The maximum angle subtended was approximately 9°, giving an energy range of 26 keV for the 2.5 MeV neutrons and 35 keV for the 5.0 MeV neutrons. All dosemeter holders were placed adjacent to each other, however, they are reasonably small and lightweight so that scatter between them is not a problem, particularly since the response of the dosemeters is very low for neutron incidence at 90° to the normal.

After irradiation, all dosemeters were returned to the issuing service for processing. The data set returned by the service detailed the "tracks per area read" for both the irradiated dosemeters and also for those used as controls. From these data, and a knowledge of the area read, the net track density, i.e., gross tracks minus control tracks, was calculated for each irradiated dosemeter. No measure of the uncertainty in the track density values was supplied.

Figure 1 shows the fluence response derived from the three multi-energy field irradiations, covering the energy range 100 keV to 1.2 MeV, and the data are presented separately for each of the PADC sheets A, B, C, and D. Each individual plot shows the results, for dosemeters positioned on both sides of the support ring. This allows a comparison of the results for dosemeters at positive and negative angles upon the support ring in order to provide a check on the symmetry of the irradiation system. The data clearly show that there is no measurable bias in that the results for positive angles match those for negative angles extremely well. For the elements from each sheet the results show a very smooth variation of fluence response with neutron energy. There is, however, some evidence of greater variability, i.e. larger uncertainties, for the results at higher energies around about 1 MeV.

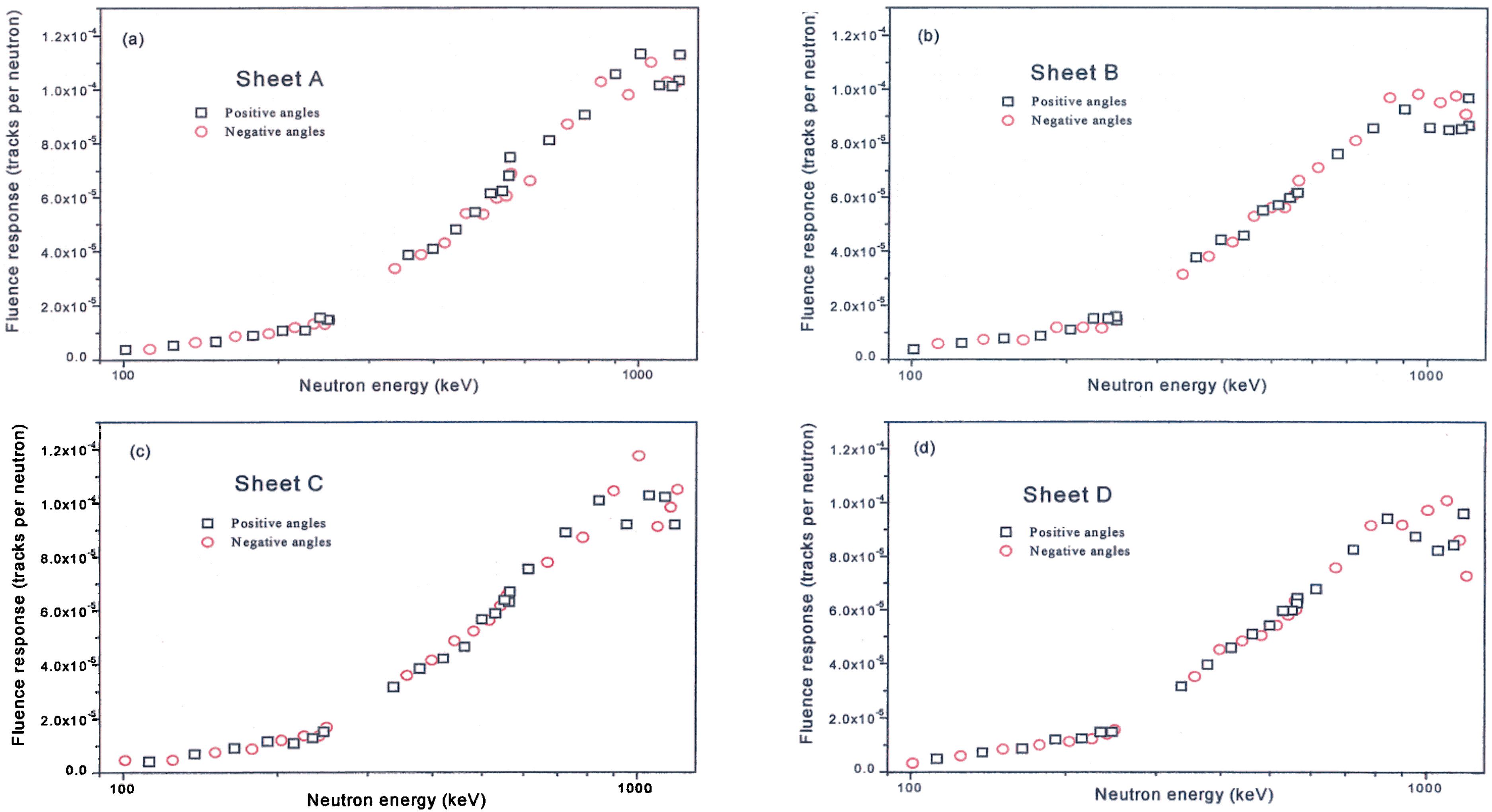

Figure 1. Comparison of the fluence response for positive and negative angles on the ring for the individual sheets of PADC for dosemeter set P1

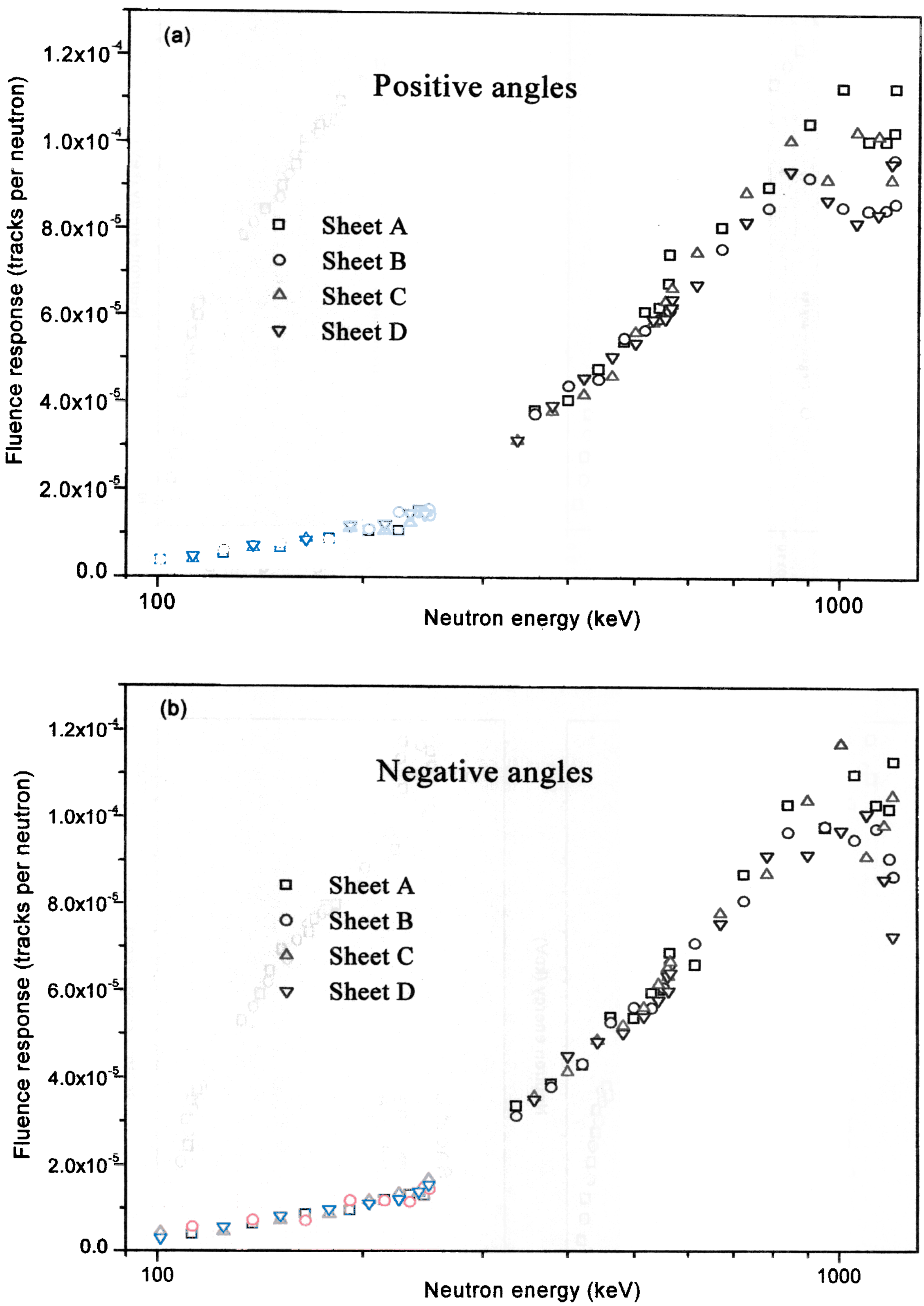

Figure 2. Comparison of dosemeter fluence response for set P1 for the different sheets of PADC

Figure 2 shows the variability of the results between the different sheets, again only using the fluence response values measured with the three multi-energy fields. The results have been plotted for the positive and negative angles separately to avoid making the figure too complicated. Once again it can be seen that the variation of response with energy is very smooth. The greater variability of the results around 1 MeV, noted above for the data as plotted in Figure 1, is, if anything, even more apparent. Some of this variation at these higher energies appears to be due to inter-sheet variation with results for sheets B and D being consistently lower than A and C. This dependence on the sheet is not apparent at lower energies, even within the data set for the energy region 561 keV to 1.2 MeV, and therefore looks to be a property of the dosemeters and/or their processing and reading rather than of the experiment.

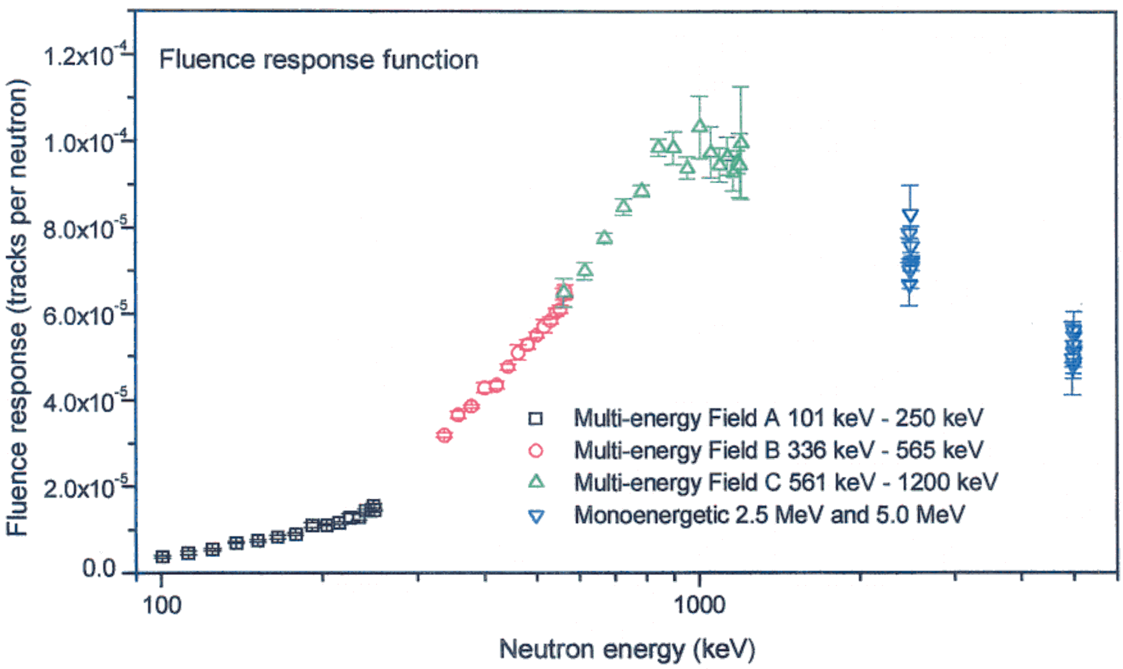

Figure 3. Fluence response function for dosemeter set P1

Figure 3 shows an averaged fluence response value for all dosemeters irradiated at each energy using the multi-energy facility. This corresponds to four dosemeters at each energy value except the highest energy in each of the multi-energy fields. This corresponds to the 0° angle on the support ring which only contained two dosemeters. The error bars shown were derived simply from the spread of the four (or two) results at each energy.

Also plotted on this figure are the results from the monoenergetic neutron measurements at 2.5 MeV and 5.0 MeV. For these irradiations the dosemeters were distributed on the phantom surface in such a way that sets of dosemeters were arranged at the same distance from the centre of the phantom face. All dosemeters within a set, and a set consisted of 2 or 4 dosemeters, were thus bombarded with neutrons at the same angle relative to the proton bombarding beam, and hence with neutrons of the same energy. The variation of energy over the phantom surface amounted to at most 1% but, for completeness, the dosemeters in each set, and there were eight sets in all, were analysed separately. A datum for each set is plotted in Figure 3, and also the uncertainty derived from the spread within the set.

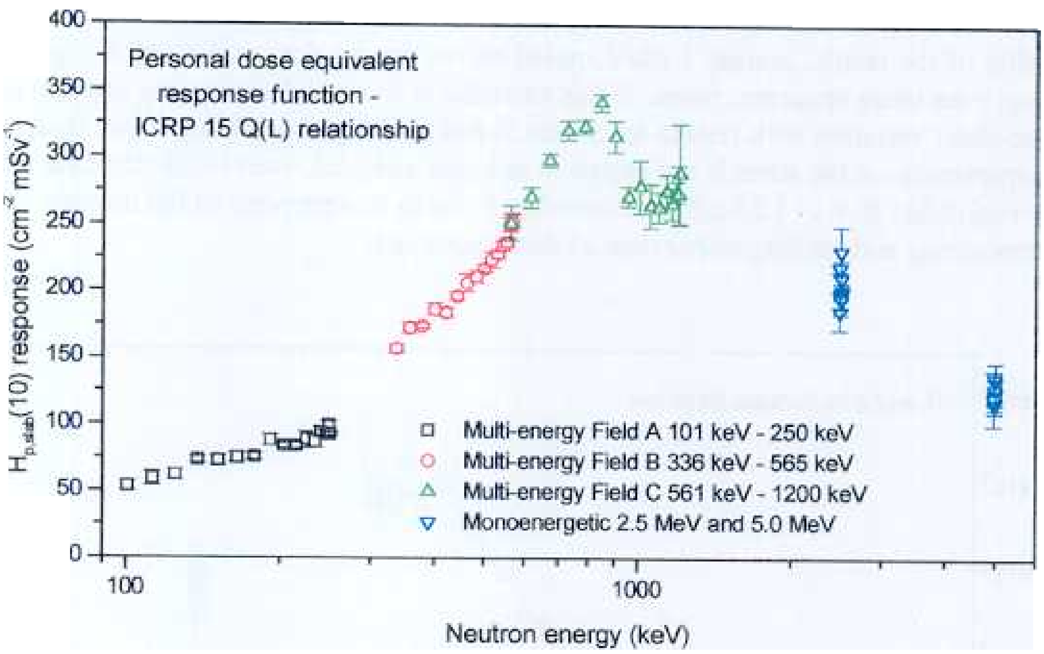

Figure 4. Personal dose equivalent response function for dosemeter set P1

Finally, Figure 4 shows the personal dose equivalent response function, i.e. the net track density per unit personal dose equivalent (cm^{-2} mSv^{-1}). The dose equivalent response function is slightly less smooth than that for the fluence, and this reflects some lack of smoothness in the conversion coefficients as a function of energy. These have been derived using Monte Carlo transport calculations, which have statistical uncertainties, and they may also reflect genuine structures in the cross sections used in the calculations.

3.2 Dosemeter set P2

Dosemeter set P2 included sensor elements from two somewhat different types of PADC plastic, in that they were obtained by the service from two different suppliers. They were designated Type I and Type II. Each dosemeter was labelled with its type, and an identifying number. The sensor elements were not supplied in the conventional configuration of one sensor element per dosemeter. Each dosemeter in fact contained six sensor elements, three elements adjacent to the front face, and three elements adjacent to the back face with an irradiator between the two sets of elements. The irradiator consisted of a thin piece of polyethylene, about 1 mm thick, which was in close contact with the sensor. A further three sensor elements were attached to the back of the dosemeters with double-sided adhesive tape with an irradiator adjacent to the back face of the dosemeter. However the elements on the back of the Type I dosemeters were not part of the measurement but acted only as a spacer, allowing the front face of both dosemeters to be the same distance from the neutron source during the irradiations. Figure 5 shows the configuration and identifying name given to each layer of sensor elements. The terms ‘bottom’, ‘middle’, and ‘top’ were assigned by the service. They derive simply from the way in which the configuration was assembled, and in fact the bottom array was the one closest to the neutron source during an irradiation.

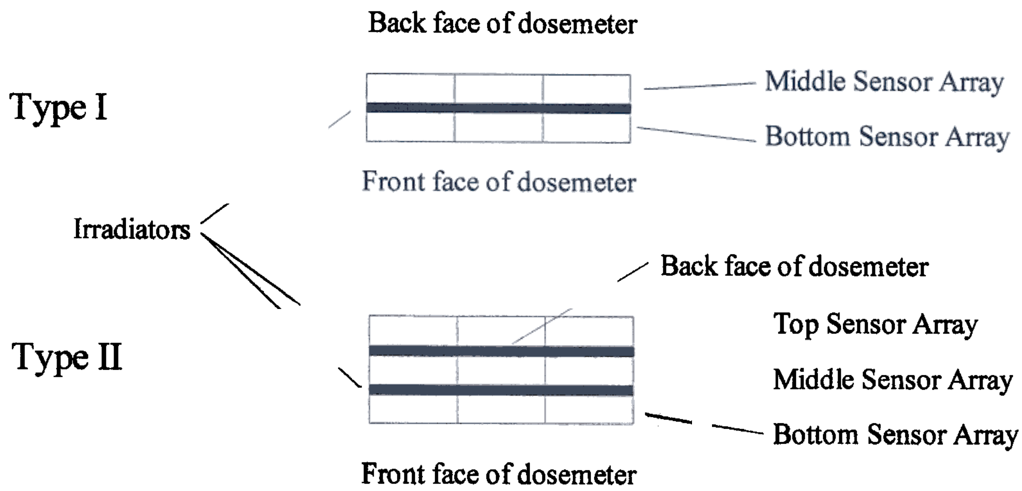

Figure 5. Plan view showing the configuration of the sensor elements for both types of dosemeter and the identifying name given to each layer of sensor elements.

There were 31 dosemeters of each type, for each of the three multi-energy fields, and 6 dosemeters of each type for the monoenergetic neutron energies, 2.5 MeV and 5.0 MeV. A further 8 dosemeters of each type were supplied to act as controls; 7 being associated with the dosemeters used for the multi-energy field measurements, and 1 with those used for the monoenergetic measurements.

The arrangements for mounting the dosemeters was similar to that for set P1. For each of the multi-energy fields a dosemeter containing elements of each type was placed at each post on the support ring, and these were positioned at 5° intervals from -75° through 0° to +75° . The arrangement for mounting the dosemeters at each position upon the support ring involved firstly attaching the two dosemeters to a strip of card with double-sided adhesive tape. An elastic band was then used to hold each card in place on the support post in such a way that one dosemeter was above the plane defined by the bombarding proton beam, and the other was the same distance below. Both dosemeters on a given post were thus irradiated with neutrons of the same energy and fluence. Type I dosemeters were positioned above the horizontal plane and the Type II below the horizontal plane. Irradiation of the dosemeters followed the procedure outlined in section 2.1 The reference point for calculation of the fluence for each sensor array was the back of the sensor as outlined in section 2.4

For irradiation with neutrons of 2.5 and 5.0 MeV, Type I and Type II dosemeters were irradiated separately. For each type, the 6 dosemeters were supplied attached to a card in 2 columns of 3 rows. The dosemeters had a vertical separation between them of 14 mm and a horizontal separation of 5 mm. The card was attached to the phantom with doubled sided adhesive tape such that the dosemeters were symmetrical about the centre of the phantom. The maximum angle subtended was approximately 1.5°, giving an energy range of 2.5 keV for the 2.5 MeV neutrons and 3.4 keV for the 5.0 MeV neutrons.

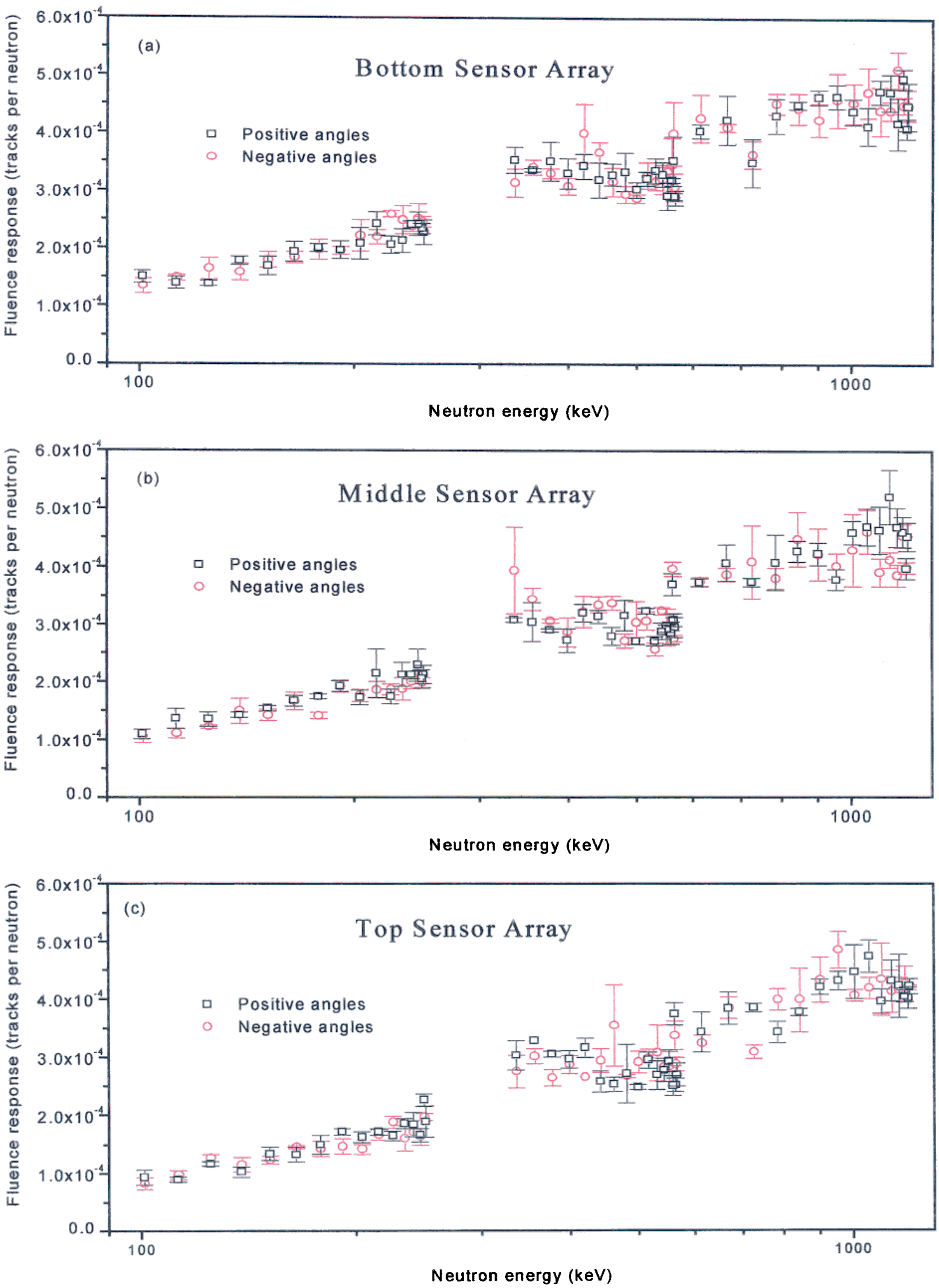

Figure 6. Comparison of positive and negative angles for the three arrays of dosemeter set P2

After irradiation all dosemeters were returned to the issuing service for processing. Unfortunately, the data set returned contained results for the Type II dosemeters only. Discussion with the service revealed that the Type I dosemeters were an experimental batch, and the results proved so variable that they were unusable. The data set received detailed the gross track density for the irradiated Type II sensor elements, and also for the Type II controls. From these data the net track density, i.e., gross tracks minus control tracks, was calculated for each irradiated sensor element. No measure of the uncertainty in the track density values was supplied.

Figure 6 shows the fluence response derived from the three multi-energy field irradiations, covering the energy range 100 keV to 1.2 MeV. The results are presented separately for the three sensor arrays, top, middle and bottom. The plotted points represent an average of the three sensor elements in each array, and the error bars shown were derived simply from the spread of the three results at each energy. Each individual plot shows results for dosemeters positioned on both sides of the support ring. This allows a comparison of the results for dosemeters at positive and negative angles upon the support ring in order to check on the symmetry of the irradiations. The data clearly show that there is no measurable bias in the results since the results for positive angles match those for negative angles extremely well.

For a small number of the points plotted in Figure 6 the error bars are particularly large. Since the uncertainties were derived from the spread of only three data values, some degree of variation is expected in the size of the uncertainties - simply because of the rather small sample. However, the large error bars often coincide with points which are higher than their neighbours. The high mean value and large spread were in most cases the result of the reading of one single sensor element being high.

At the lowest energies the bottom sensors, i.e. those closest to the neutron source, show a higher response than the sensors further away. The manner in which the neutron fluence is calculated, by taking the irradiation distance to be that to the rear surface of an array, ensures that correct allowance is made for differences in the fluence at the various arrays resulting from the inverse square dependence of the fluence on distance. However, no allowance is made for attenuation in the sensors closer to the neutron source. This attenuation increases as the energy decreases, so its effects should be most noticeable at low energies. At higher energies the effects of attenuation are expected to be less prominent, and this is the case.

Perhaps the most noticeable feature of the data is that the results for multi-energy Field B (336 keV to 565 keV) do not fit in particularly well with those for fields A and C. Field B results show, if anything, a slight decrease in fluence response with increasing neutron energy. To date, no explanation for this feature has been found despite extensive investigation. The service can find no errors in the reading of the dosemeters. The relative fluence values at the different angles have been checked carefully, and no errors can be found. Field B provides the highest fluence rates, but, because the irradiation times were shorter, the highest track densities for Field B were only about 10% greater than the highest track densities for Field A. Thus, overlapping tracks on the sensor elements, and hence missed tracks, should not have been a problem for Field B if it was not one for Field A. Furthermore this effect, although it might cause the high energy response values to be lower than they should be, would not explain the high responses at the lower energies around 340 keV. The high fluence rate for Field B meant that two sets of dosemeters could be irradiated on the same day. There was, however, no evidence of the same problem with the other set irradiated on the same day as set P2.

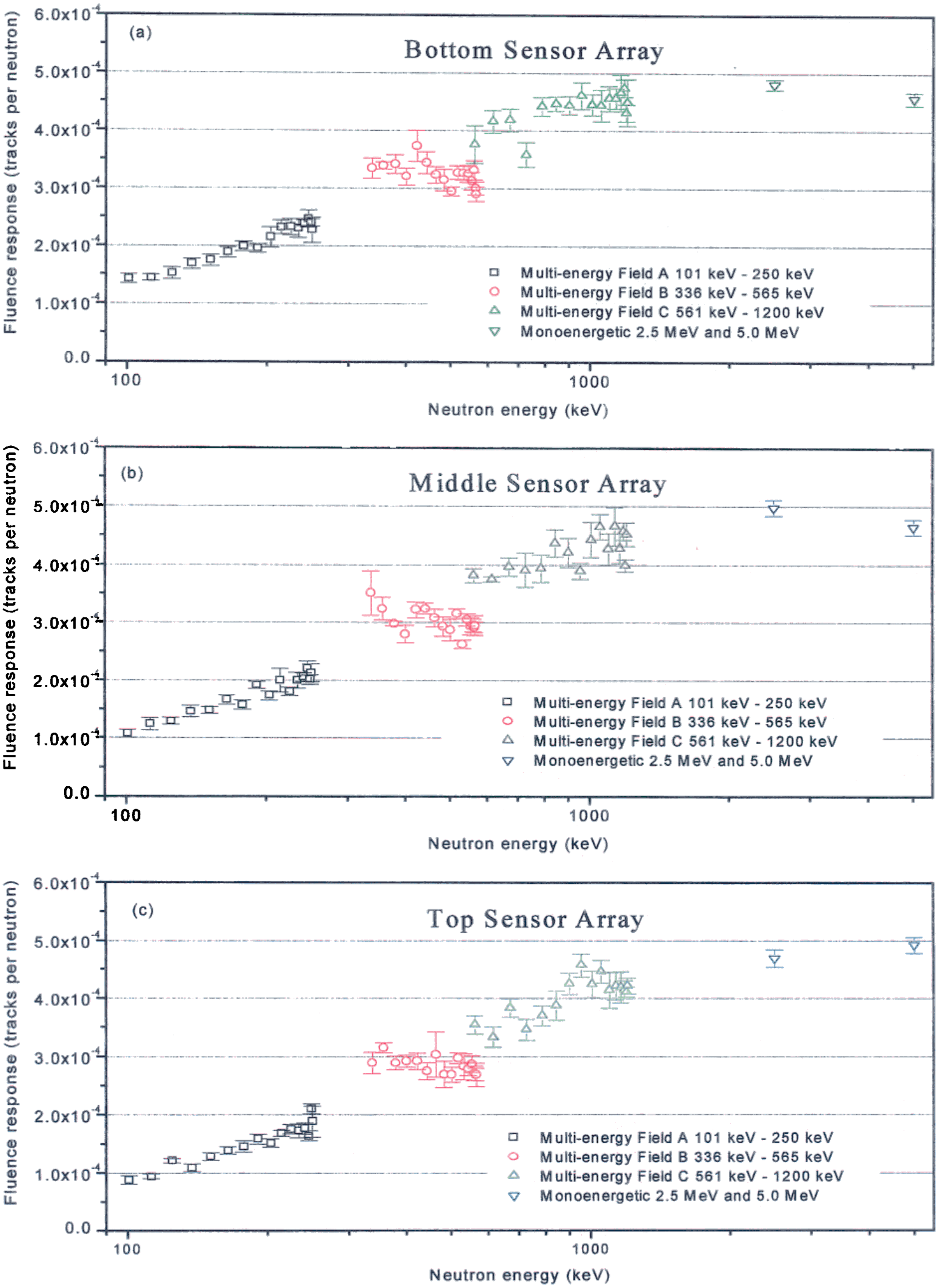

Figure 7. Fluence response functions for the three arrays of sensors of dosemeter set P2

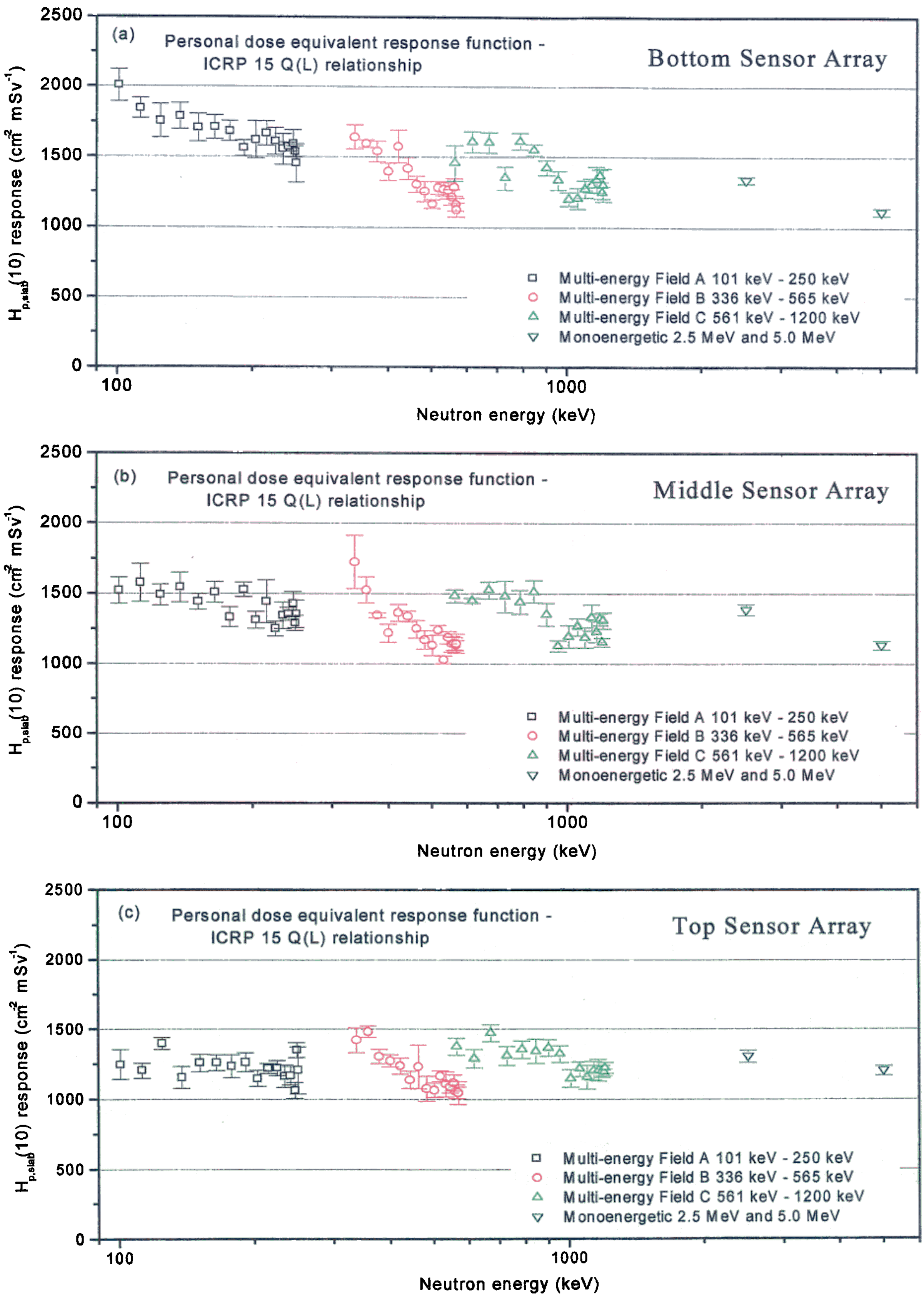

Figure 8. Personal dose equivalent response functions for the three arrays of sensors of set P2

Figure 7 shows the averaged fluence response value for all sensor elements irradiated at each energy using the multi-energy facility, i.e. the positive and negative angles have been averaged. The data are still presented separately for the three sensor arrays, top, middle and bottom. The plotted points correspond to six sensor elements at each energy, except the highest energy in each of the multi-energy fields. This corresponds to the 0° angle on the support ring which contained only one dosemeter of each type. The error bars shown were derived simply by the spread of the six (or three at 0°) results at each energy.

Also plotted on the figure are the results from the monoenergetic neutron measurements at 2.5 MeV and 5.0 MeV. Although for these irradiations the dosemeters were distributed over the phantom face, they were all reasonably close to the centre, and the variation of energy for different dosemeters amounted to at most 0.1%, which was considered to be negligible. Therefore all the elements within an array were averaged for all dosemeters, this amounted to 18 elements for the 2.5 MeV measurements, and 15 elements for the 5.0 MeV measurements because the results for one of the latter dosemeters were not returned. The error bars shown were derived simply form the spread of the results at each energy.

Figure 8 shows the personal dose equivalent response function, i.e. the net tracks density per unit personal dose equivalent (cm^{-2} mSv^{-1}) . The data are presented separately for the three sensor arrays, top, middle and bottom. As in Figure 7, the plotted points represent mean values for six sensors, except those corresponding to 0°, and the error bars derive solely from the spread of the data.

3.3 Dosemeter set P3

Sensor elements for dosemeter set P3 were cut from a number of nominally identical sheets of PADC plastic all obtained from the same manufacturer. Dosemeters from three sheets, designated A, B, and C, were used for irradiations in the multi-energy fields A, B, and C respectively. There were 31 dosemeters for each multi-energy field. Also supplied were 2 dosemeters for each of the monoenergetic neutron energies, 2.5 MeV and 5.0 MeV, and 6 dosemeters to act as controls. No information was provided on the sheet, or sheets, from which these latter 10 dosemeters originated. Each dosemeter was labelled with a unique serial number, and contained 2 sensor elements, both being in the same plane, and parallel with the back surface of the dosemeter. For the monoenergetic irradiations the pattern for positioning the dosemeters on the phantom face was suggested by the service.

For each of the multi-energy fields, one dosemeter was placed at each post on the support ring, and the posts were positioned at 5° intervals from -75° through 0° to +75° . An elastic band was used to hold each dosemeter in place on the support post in such a way that one sensor element was above the plane defined by the bombarding proton beam, the other below. Both sensor elements in a given dosemeter were thus irradiated with neutrons of the same energy and fluence. Irradiations followed the procedure outlined in section 2.1

For irradiation with 2.5 and 5.0 MeV monoenergetic neutrons, two dosemeters were attached to the phantom with doubled sided adhesive tape. One dosemeter was positioned in the left quadrant above the horizontal plane defined by the bombarding proton beam, the other dosemeter in the right quadrant below this plane. This configuration minimises the effects of scatter between dosemeters. The dosemeters of set P3 are rectangular, and the 2 PADC sensor elements which are processed to obtain the track numbers are located towards one end of the rectangle. The

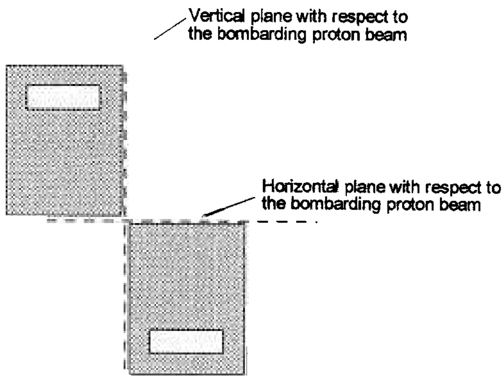

Figure 9. Showing the orientation of dosemeters on the phantom for the monoenergetic irradiations.

dosemeter positioned above the horizontal plane was therefore orientated with this end downwards, while the dosemeter below this plane was orientated in the opposite way so the processed areas of PADC had the same offset with respect to the height of the source of neutrons. Both dosemeters were thus irradiated with neutrons of the same energy and fluence, see Figure 9.

After irradiation, all dosemeters were returned to the issuing service for processing. The data set returned by the service detailed the gross track density and net track density for both the irradiated dosemeters and also those used for the controls. No data was supplied for the numbers of tracks on individual sensor elements within each dosemeter, and no measure was provided of the uncertainty in the track density values.

Figure 10 shows the fluence response derived from the three multi-energy field irradiations, covering the energy range 100 keV to 1.2 MeV. The plot shows these results for dosemeters positioned on both sides of the support ring thus allowing a comparison of the results for dosemeters at positive and negative angles upon the support ring. The data clearly show that there

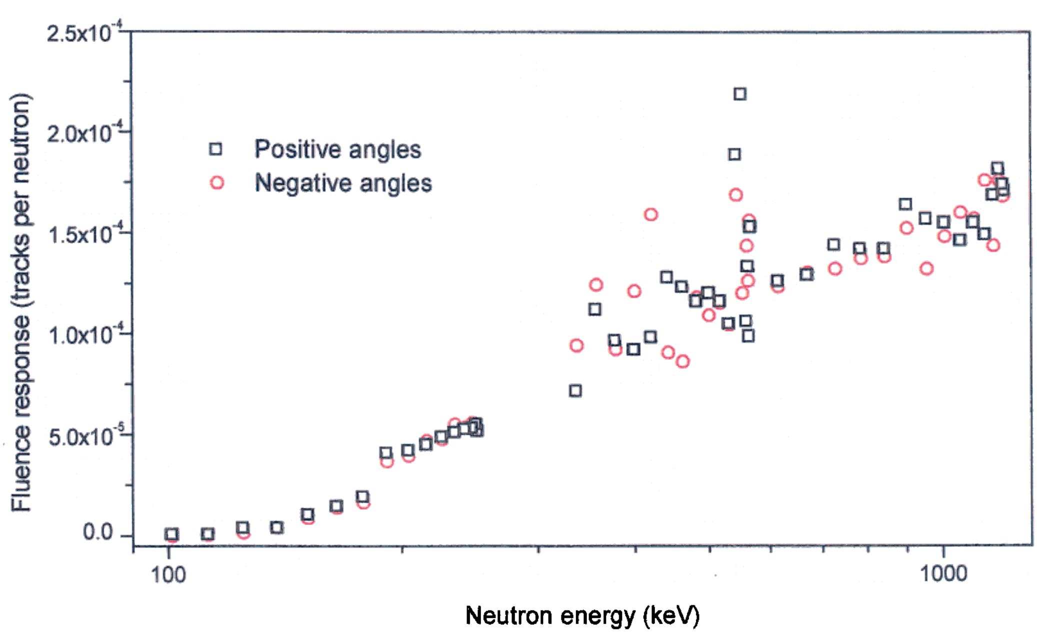

Figure 10 Comparison of fluence response for positive and negative angles on the ring for set P3

is no measurable bias in the results since those for the positive angles match those for negative angles extremely well. The most notable feature of the data are some rather high response values which occur for the multi-energy field B (336 keV to 565 keV). Although the overall trend of the variation with energy fits in well with the data from Fields A and C, the data points show a greater dispersion than exhibited for the other two fields. To date, no explanation for this feature has been found despite extensive investigation. The service can find no errors in the reading of the dosemeters and has in fact has re-read a number of the dosemeters.

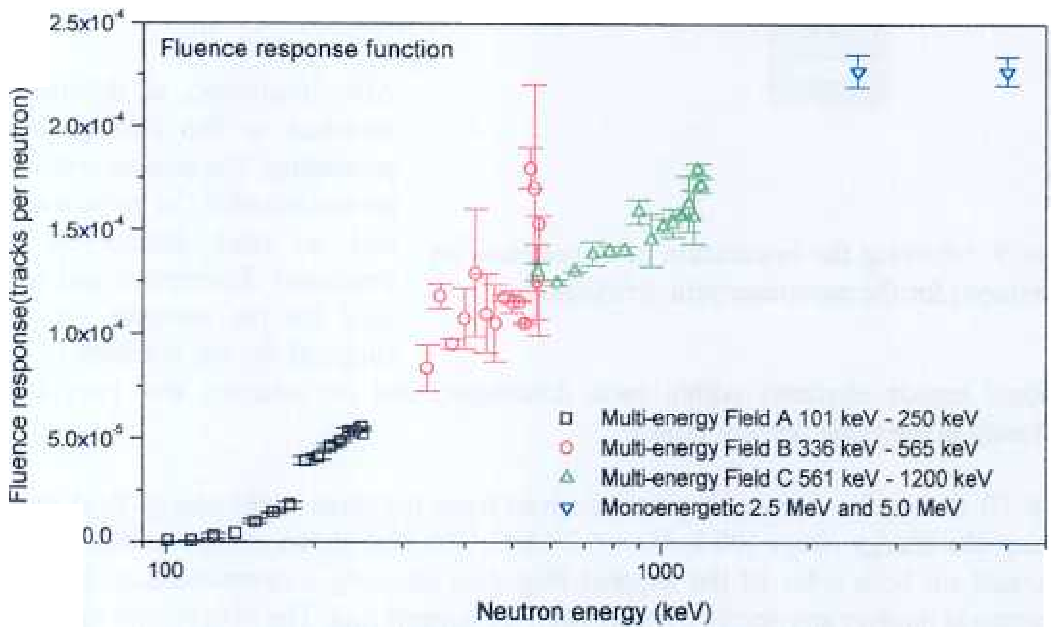

Figure 11 Fluence response function for dosemeter set P3

Figure 11 shows an averaged fluence response value for all dosemeters irradiated at each energy using the multi-energy facility. The values correspond to two dosemeters at each energy value except the highest energy in each of the multi-energy fields. The error bars shown were derived simply from the spread of the two results at each energy, and there are thus no error bars associated with the single dosemeter results corresponding to 0° angle on the support ring. Since the uncertainties were derived from just two readings their values are likely to be very variable, and they only represent a very rough idea of the uncertainty for an individual datum. However, their average value should represent a reasonable measure of the typical uncertainty. The combined data from the three multi-energy fields show a smooth trend with energy, and since the PADC elements for each field were derived from a different sheets of plastic, this indicates that there are no gross variations between the three sheets.

Several, although not all, of the response values which are higher than the trend of the others also have large uncertainties indicating that the effect was due to one dosemeter at one angle reading high.

Also plotted on the figure are the averaged fluence response for the monoenergetic neutron measurements at 2.5 MeV and 5.0 MeV. The error bars shown were derived simply from the spread of the results for the dosemeters irradiated at each energy.

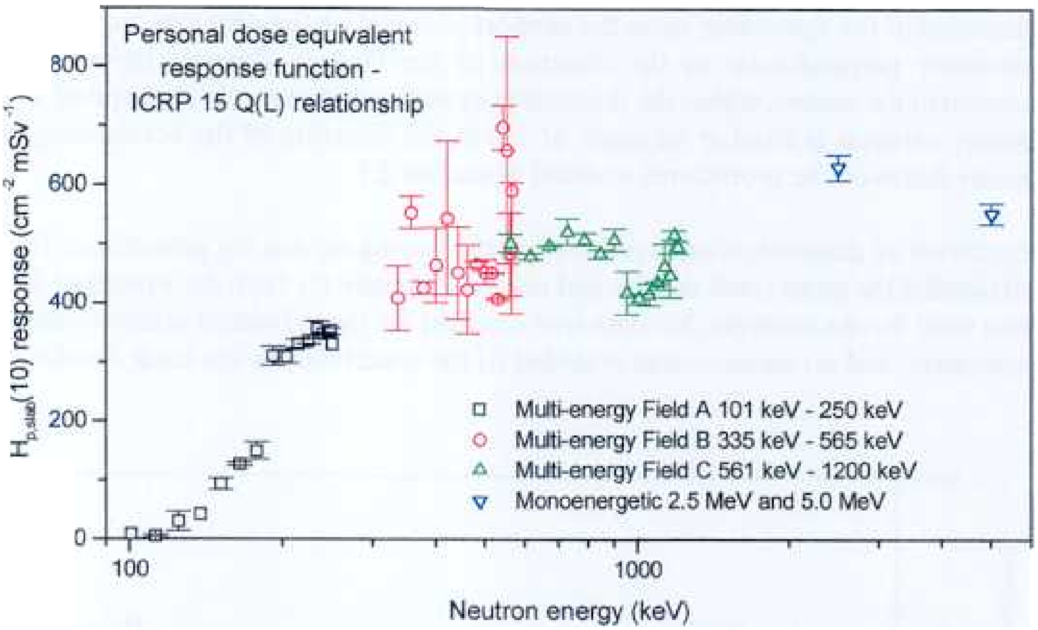

Figure 12. Personal dose equivalent response function for dosemeter set P3

Figure 12 shows the personal dose equivalent response function, i.e. the net tracks density per unit personal dose equivalent (cm^{-2} mSv^{-1}) . As noted for other services, the dose equivalent response function is slightly less smooth than that for the fluence, reflecting the lack of smoothness in the conversion factors as a function of energy.

3.4 Dosemeter set P4

Dosemeter set P4 again included PADC sensor elements from a number of sheets of plastic. All of the sheets were from the same manufacturer, and hence were nominally identical. Three sheets, designated numbers 1, 2, and 3, were used for the irradiations in the multi-energy fields A, B, and C, respectively, and 31 dosemeters were provided for each multi-energy field. Also supplied were a single dosemeter for each of the monoenergetic neutron energies, 2.5 MeV and 5.0 MeV, and 2 dosemeters to act as controls. The sheet, or sheets, from which these latter 4 dosemeters originated were not specified. Each dosemeter was labelled with a unique serial number. The dosemeters were circular in shape with a flat rear face, and a domed front. Each one contained 3 sensor elements equally spaced on a triangular foam pyramid. The angle subtended between the sensor and the rear face of the dosemeter is approximately 35°. The orientation of the pyramid within the dosemeter is not fixed and was therefore completely random from one dosemeter to the next.

For each of the multi-energy fields one dosemeter was placed at each post on the support ring, and the posts were positioned at 5° intervals from -75° through 0° to +75°. The dosemeters incorporated a plastic clip on the rear face which was used to attach it in place on the support post. The dosemeters were positioned such that they were bisected by the horizontal plane defined by the bombarding proton beam. For irradiation with the mono-energetic neutrons the single dosemeter was attached to the centre of the phantom with doubled sided adhesive tape.

The orientation of the dosemeter upon the support post and on the phantom has the rear face of the dosemeter perpendicular to the direction of the neutron fluence. However, with the configuration of the sensors within the dosemeter as outlined above - in the shape of a pyramid - each sensor element is fixed at an angle of 55° to the direction of the bombarding neutrons. Irradiations followed the procedures outlined in section 2.1

After irradiation all dosemeters were returned to the issuing service for processing. The data set returned detailed the gross track density and net track density for both the irradiated dosemeters and those used for the controls. No data was supplied for the individual sensor elements within each dosemeter, and no measure was provided of the uncertainty in the track density values.

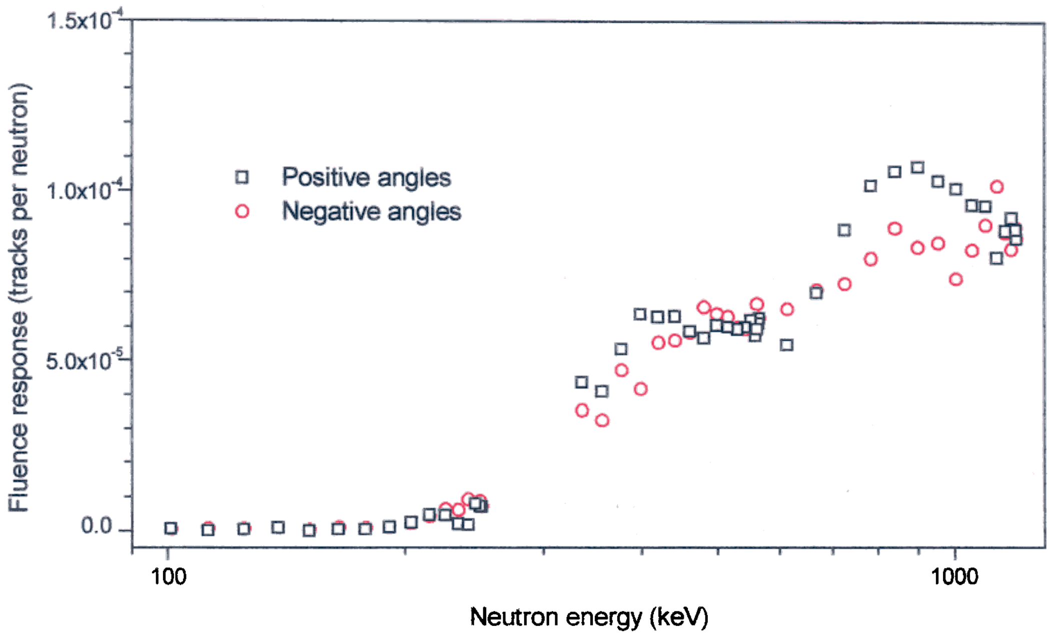

Figure 13. Comparison of fluence response for positive and negative angles for set P4

In Figure 13 the fluence response values derived from the three multi-energy field irradiations, covering the energy range 100 keV to 1.2 MeV are plotted separately for dosemeters positioned on both sides of the support ring. The data for Fields B and C appear to show a lack of symmetry between the positive and negative angles on the ring; an effect which was not present in the results for dosemeter sets P1, P2, or P3. Field C results, in particular, show on average a noticeably higher fluence response for those dosemeters on the positive side of the support ring. However there is good agreement near 0° and at the larger angles. Without information on the uncertainties in individual dosemeter readings, however, it is difficult to determine the significance of these differences. To date, no explanation for this feature has been found despite extensive investigation.

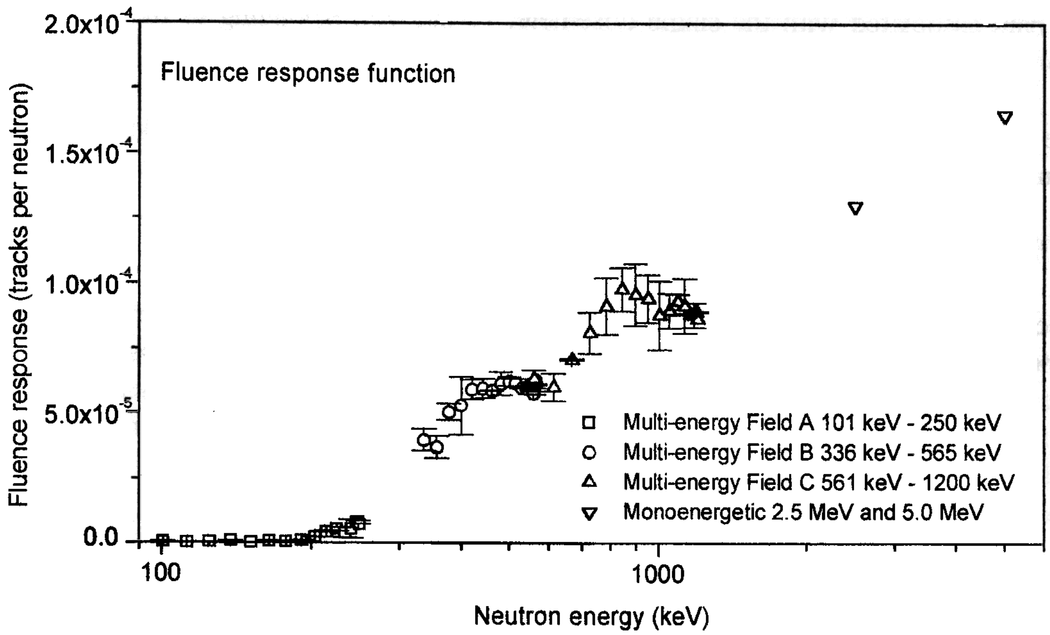

Figure 14. Fluence response function for dosemeter set P4

Figure 14 shows an averaged fluence response value for all dosemeters irradiated at each energy using the multi-energy facility. These values correspond to two dosemeters at each energy except the highest energy in each of the multi-energy fields. Also plotted on the figure are the fluence response for the monoenergetic neutron measurements at 2.5 MeV and 5.0 MeV. The error bars

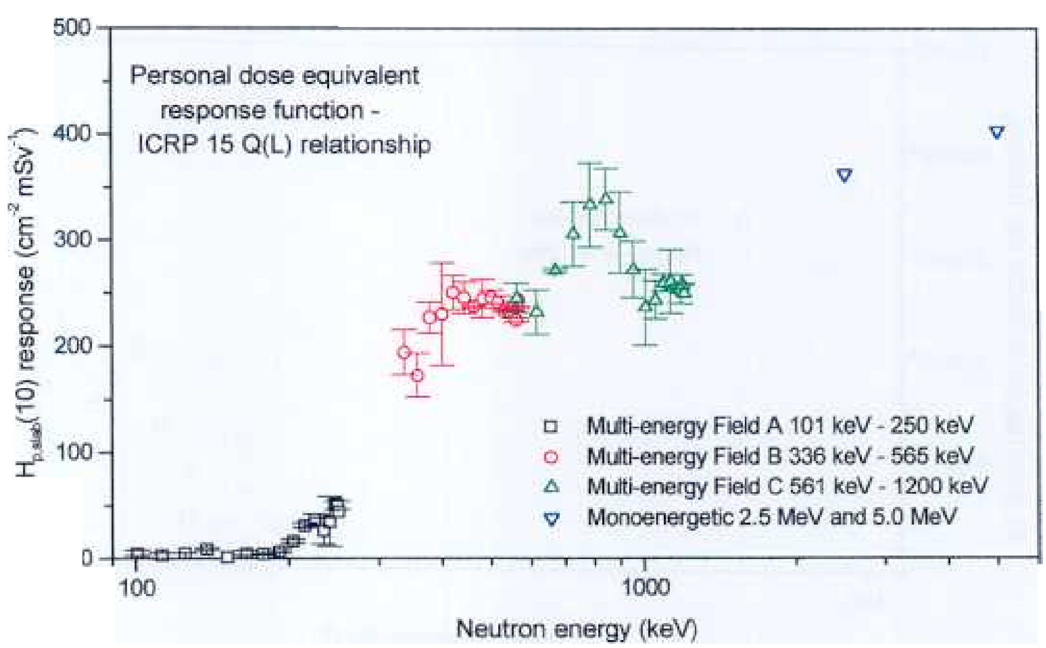

Figure 15. Personal dose equivalent response function for dosemeter set P4

shown were derived simply from the spread of the two results at each energy. There are thus no error bars associated with the single dosemeter results corresponding to the 0° angle on the support ring, or with the monoenergetic measurements on the phantom.

Figure 15 shows the personal dose equivalent response function, i.e. the net tracks density per unit personal dose equivalent (cm^{-2} mSv^{-1}) .

3.5 Dosemeter set N1

The sensor elements for dosemeter set N1 were NTA film packages. The service provided 31 dosemeters for irradiation in multi-energy Field C (561 keV to 1200 keV), 9 dosemeters for each of the monoenergetic neutron energies, 2.5 MeV and 5.0 MeV, and 6 dosemeters to act as controls. Each dosemeter was labelled with a unique serial number, and contained a single NTA film element. For the monoenergetic irradiations the relative positions on the phantom face were indicated by the service.

For irradiation in multi-energy Field C one dosemeter was placed at each post on the support ring, and the posts were positioned at the usual 5° intervals. An elastic band was used to hold each dosemeter in place on the post in such a way that the sensor element was bisected by the horizontal plane defined by the bombarding proton beam. Irradiations followed the procedure outlined in section 2.1

For irradiation with the 2.5 and 5.0 MeV monoenergetic neutrons, the dosemeters were attached to the phantom with doubled sided adhesive tape. For each of these two energies the 9 dosemeters were attached to the phantom in a 3 column by 3 row array. The dosemeters had a vertical separation of 15 mm, and also a horizontal separation of 15 mm. The angle subtended by the

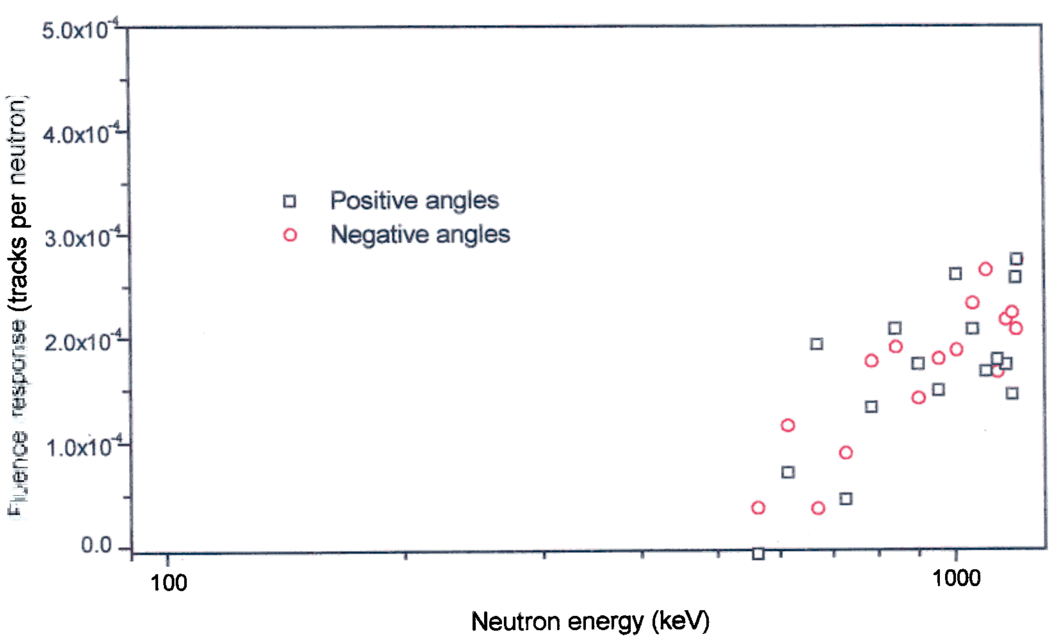

Figure 16. Comparison of fluence response for positive and negative angles for set N1

dosemeter furthest from the centre of the phantom face was approximately 7.5°; giving an energy spread of 18 keV for the 2.5 MeV neutrons, and 24 keV for the 5.0 MeV neutrons.

After irradiation all dosemeters were returned to the issuing service for processing. The data set returned by the service detailed the gross track density for both the irradiated dosemeters and those used as controls. From these data the net track density was calculated for each irradiated dosemeter. No measure of the uncertainty in the track density values was supplied.

Figure 16 shows the results for that part of the fluence response function curve covered by multi-energy Field C. The plot shows the results for dosemeters positioned on both sides of the support ring, and the data clearly show that there is no measurable bias between results from the two sides.

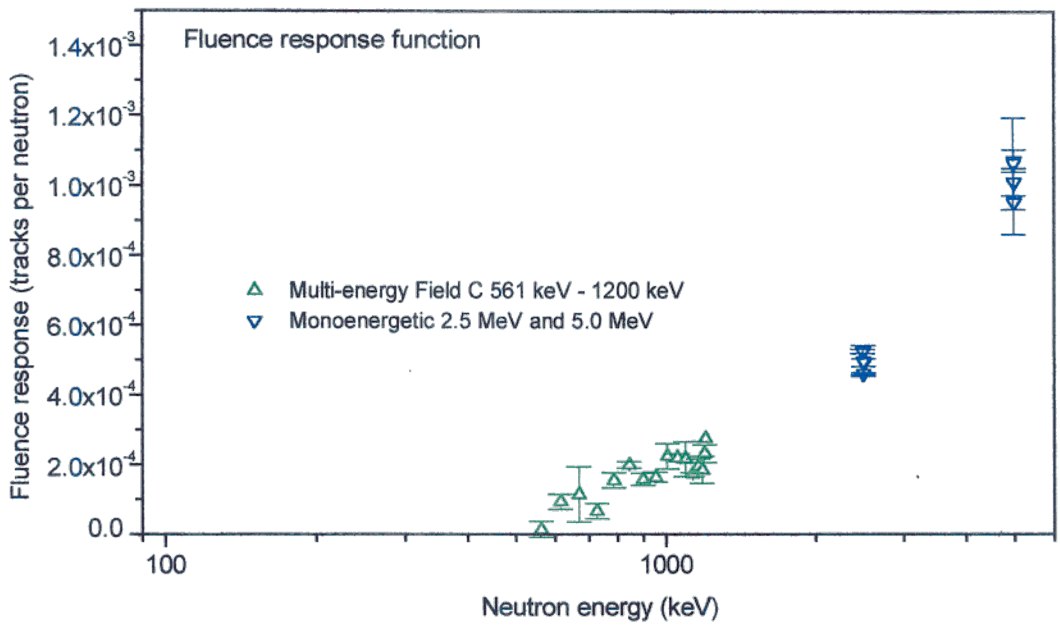

Figure 17. Fluence response function for dosemeter set N1

Figure 17 shows an averaged fluence response value for all dosemeters irradiated at each energy using the multi-energy facility. The values were derived using the two dosemeters at each energy value, except for the highest energy. The error bars shown were derived simply from the spread of the two results at each energy.

Also plotted on the figure are the averaged fluence response for the monoenergetic neutron measurements at 2.5 MeV and 5.0 MeV. For these irradiations the dosemeters were distributed on the phantom surface in such a way that pairs of dosemeters were positioned at the same distance form the centre of the phantom, the exception being the single dosemeter at the centre. Both dosemeters of each pair were bombarded with neutrons at the same angle relative to the proton bombarding beam, and hence with neutrons of the same energy. The variation of energy over the phantom surface amounted to at most 1%, but for completeness the dosemeters in each pair, and there were four pairs, were analysed separately. A datum for each pair, and for the single dosemeter at the centre is plotted in Figure 17, together with the uncertainty derived from the spread of each pair.

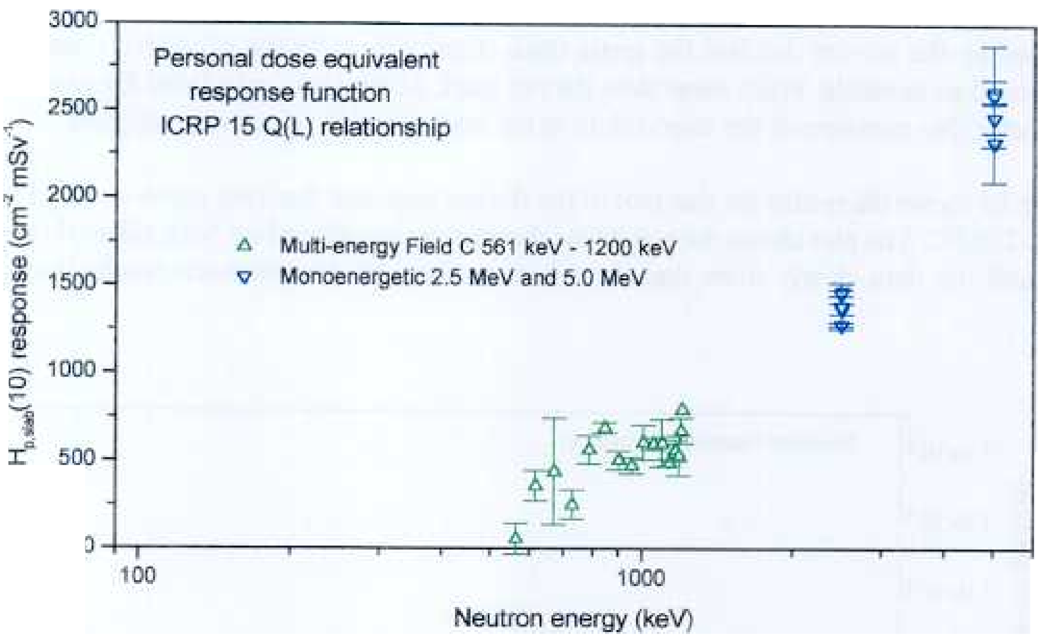

Figure 18. Personal dose equivalent response function for dosemeter set N1

Figure 18 shows the personal dose equivalent response function.

3.6 Dosemeter set N2

Dosemeter set N2 used NTA film as the sensor element. Irradiations were performed of 31 dosemeters on the ring for multi-energy Field C, and 9 dosemeters were irradiated on phantom at 2.5 MeV, and 9 at 5.0 MeV. No results have, however, been returned by the service. They have been contacted a number of times, but to date no response data has been reported to the authors.

4. DISCUSSION

4.1 The effects of scattering in the neutron-producing target assembly

The nominally monoenergetic neutrons produced at a particular angle, when using an accelerator beam to bombard a neutron-producing target, always have a contaminating component resulting from neutron scattering in the target can assembly. This effect has been studied in detail[(16)], both experimentally and computationally, at the German National Standards Laboratory, PTB. Using a Monte Carlo computer program, obtained from the PTB, the spectra of the scattered neutrons were calculated for all the bombarding conditions used in this work. The calculated total scatter components are shown in Table 2 as a percentage of the 0° fluence.

Table 2. Target scatter, as a percentage of the 0° fluence, for the reactions used in this work.

0° energy	Reaction	Scatter fraction
250 keV	$^{7}Li(p,n)^{7}Be$	2.7%
565 keV	$^{7}Li(p,n)^{7}Be$	0.9%
1.2 MeV	$T(p,n)^{3}He$	
2.5 MeV	$T(p,n)^{3}He$	
5.0 MeV	$D(d,n)^{3}He$	1.0%

Certain identifiable features can be found in the spectra of the scattered neutrons. Firstly, there is a small peak at the energy corresponding to neutron emission at 90° to the bombarding beam direction. These neutrons have a long path-length in the disc forming the end of the target can, and thus have a high probability of scatter. Since the target can and target backing materials are all reasonably high atomic mass (Z≥54) the energy loss in the scattering process is small, being less than 8% even for 180° degree scattering. Above the 90° emission peak there is a continuum extending up to the 0° neutron energy. Scattering also occurs from the cylindrical part of the target can, and from the flange where it is attached to the flight tube from the accelerator. Neutrons scattered from these parts in general have even lower energies extending down to the energy corresponding to neutron emission from the target layer at 180° to the bombarding beam direction. Figure 19 shows the calculated spectrum for 2.5 MeV neutron production at 0°. The 90° neutron emission peak occurs at 1063 keV, while a peak corresponding to 180° neutron emission from the target layer can be seen at about 453 keV.

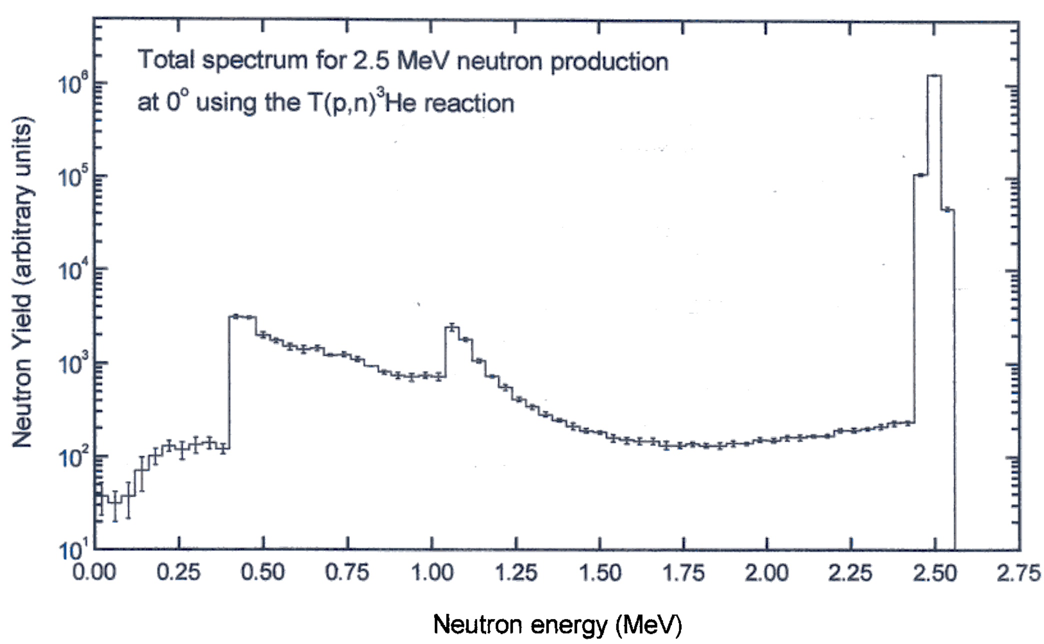

Figure 19. Fluence spectrum, including target scatter, for 2.5 MeV neutron production at 0°

The effects of target scattered neutrons on the measurements are complex. The long counter, used to measure the fluence, measures the scattered neutron component with similar efficiency to the main neutron component, so that the fluence derived from this device includes the scattered neutrons. To perform a thorough correction for the scatter the reading induced in the dosemeter by the target scattered neutrons should be calculated, using the scattered neutron spectrum and the dosemeter response function, and this should be subtracted from the measured reading. Similarly the scatter contribution to the long counter reading should be subtracted. The true dosemeter response to the monoenergetic neutrons can then be derived. This process is, of course, problematical, since the response function needed for the above procedure is the very thing which the experiment is trying to measure. An iterative approach can be used, if the accuracy required warrants this, using the uncorrected fluence measurements for the first estimate of the correction. In most cases, however, the effect of the scattered neutrons is small compared to the overall uncertainty in the measured response.

Target scatter effects can make the uncorrected results either larger or smaller than the true value. For example, in the measurement of the 250 keV response for a PADC track-etch dosemeter at 0° to the bombarding beam direction, all the target scattered neutrons have lower energies, and are thus detected with a lower efficiency since the fluence response decreases below 250 keV. Nevertheless, the detection efficiency for these neutrons is not zero, so the effect of scattering on the measured response is less than the figure for the percentage scatter fraction as given in Table 2. Conversely, for the measurement of the 101 keV response, performed at 75° to the beam direction, scattered neutrons with energies up to 250 keV can strike the dosemeter. The scattered neutrons, however, cover a wide energy range, from about 20 keV upwards. It is possible that the presence of the scatter component will have the effect of increasing the measured response, but not by more than the percentage scatter fraction at the most. The effect of scatter, even for the worst case, is thus expected to be less than about 3% for all the present measurements, and usually much less. No scatter corrections have therefore been applied, although an additional component of 3% has been added to the estimated overall uncertainties.

4.2 The PADC track-etch dosemeters

The results presented in the previous section represent, on the whole, a remarkably good and extensive set of data on PADC track-etch dosemeter response functions. For the multi-energy measurements the energy range for Field B around 0° overlaps that for Field C around 75°. Despite the very different angles, and the use of two different neutron producing reactions, there is in general excellent agreement for the results in the overlap region around 560 keV. The one exception to this is for dosemeter set P2 where the difference, which is of the order of 25%, is way outside the measurement uncertainty. No reason has yet been found for the unusual energy variation shown by the data for Field B for this dosemeter set, and a repeat of the measurements would be desirable.

Putting aside the anomalous results for dosemeter set P2 in Field B, and making allowance for the measurement uncertainties, the fluence response functions derived have, in general, a very smooth variation with neutron energy with no noticeable structure other than a very broad maximum. The exception to this is dosemeter set P4 where there is some apparent structure in the 340 keV to 1.2 MeV region. This, however, appears to be associated with the rather peculiar and unexplained asymmetry in the results for the two sides of the ring in multi-energy ranges B and C.

One other feature of the data, which occurs for several of the dosemeter sets, and particularly for Field B in set P3, is the occurrence of occasional high response values relative to neighbouring results. This is often associated with a large uncertainty value. If, when an average is taken of two or more data at a particular energy, the reading of one dosemeter is high, this affects both the mean value and the uncertainty, and this appears to have been the cause of several of the high results. Since the sheets of PADC plastic are not completely uniform, it is always possible for a single sensor element to produce a high reading due, for example, to an anomalously high background. Anomalously low readings would be more difficult to explain.

Comparing the fluence response functions for the four dosemeter sets reveals rather different shapes. Certainly no single response function shape characteristic of PADC track-etch plastic emerges. The differences presumably arise from different techniques for etching the tracks and reading the pits produced, although the characteristics of the plastics from different manufacturers must also play a part. Table 3 provides some data on the processing techniques used by the different services.

Table 3. Processing techniques used by the dosimetry services taking part in the measurements.

Dosemeter type	PADC track-etch plastic				NTA film	
	P1	P2	P3	P4	N1	N2
Processing details	Chemical pre-etch electro-chemical etch, automated counting	Chemical etch, no pre-etch, manual counting	Two stage chemical etch, automated counting	Two stage chemical etch, automated counting	Several different areas on film read manually using a microscope	Several different areas on film read manually using a microscope

A comparison of the personal dose equivalent response functions for the four dosemeter sets shows that the widely held idea of PADC track-etch dosemeters having sharp threshold in the region of 150 keV where the response drops off almost to zero is only partially true. Dosemeter set P2 appears to have a reasonably dose equivalent response all the way down to the lowest measured energy of 100 keV, and set P1 also still detects neutrons even at this low energy. These results, and those for set P2 in particular, were unexpected. There was no indication in the literature that a dose equivalent response might be expected at such low energies, and extension of the measurements to even lower energies would be desirable, and is possible.

Dosemeter sets P3 and P4 come closest to the conventional idea of a device with a threshold. For P3 this occurs fairly gradually between about 120 and 190 keV. For dosemeter set P4, in the calibration situation, the threshold is higher in the region of 300 keV. This is entirely to be expected simply because the PADC elements of set P4 are at about 55° to the incident neutrons whereas their maximum sensitivity is for normal incidence. The advantages of dosemeters of this type arise in realistic fields where the angle of incidence of the neutrons is not in general normal to the sensor element, and the pyramid arrangement provides improved angular response characteristics.

Previously measured response function data for the dosemeter sets studied here are not generally available. For sets P1 and P3, however, some earlier data were made available by the service. Those for set P1 are shown in Figure 20. They include seven monoenergetic values and results from measurements with a ^{252}Cf and an ^{241}Am-Be source. The results for the present measurements have been plotted in the same way as in Figure 4 except for the data at 2.5 and 5.0 MeV which have been plotted as single points with an uncertainty derived from the spread of all the data at each of these energies. The agreement between the previous and the present measurements is good above about 250 keV, although below this energy the earlier results are higher. Some changes to the dosemeters have taken place since the previous measurements, and the differences revealed by the figure are probably due to genuine changes in the response characteristics rather than measurement problems.

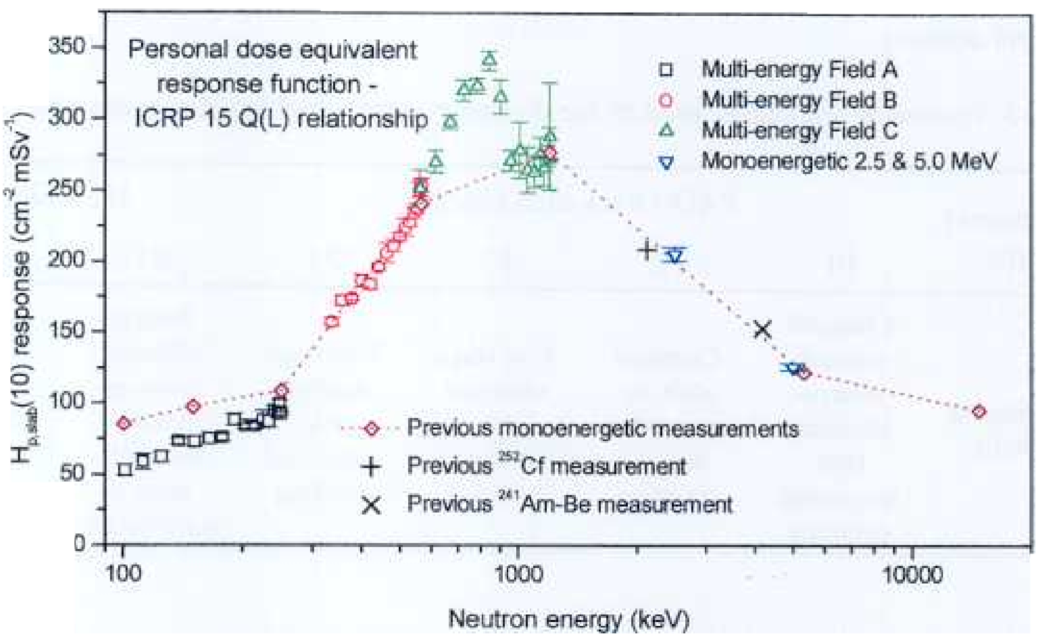

Figure 20. Comparison of present responses with earlier measurements for dosemeter set P1

The results for the two radionuclide sources have been plotted at the mean energies of their spectra. Since these spectra cover a broad energy range the values actually represent the integral, over this energy range, of the product of the response function with the spectrum. They will thus not necessarily fall on the curve representing the true response function, although they should fall reasonably close to the true response function as measured with monoenergetic neutrons.

The value of the multi-energy techniques, which provide considerably more information over the energy range 100 keV to 1.2 MeV, is highlighted by the results in the energy region just below 1 MeV. With just the previous data values at 565 keV and 1.2 MeV the extent of the peak in the response function in this region was not evident.

A comparison of previous data with the present results for dosemeter set P3 is shown in Figure 21. The previous data were derived from two sources. One set of results was provided by the service in graphical form, and an additional set of results was obtained from a recently published report[17] of a European intercomparison of nuclear track detectors. Neither of these sets of results were provided in terms of personal dose equivalent response, and the data have been converted to fluence response and are plotted in this form in Figure 21.

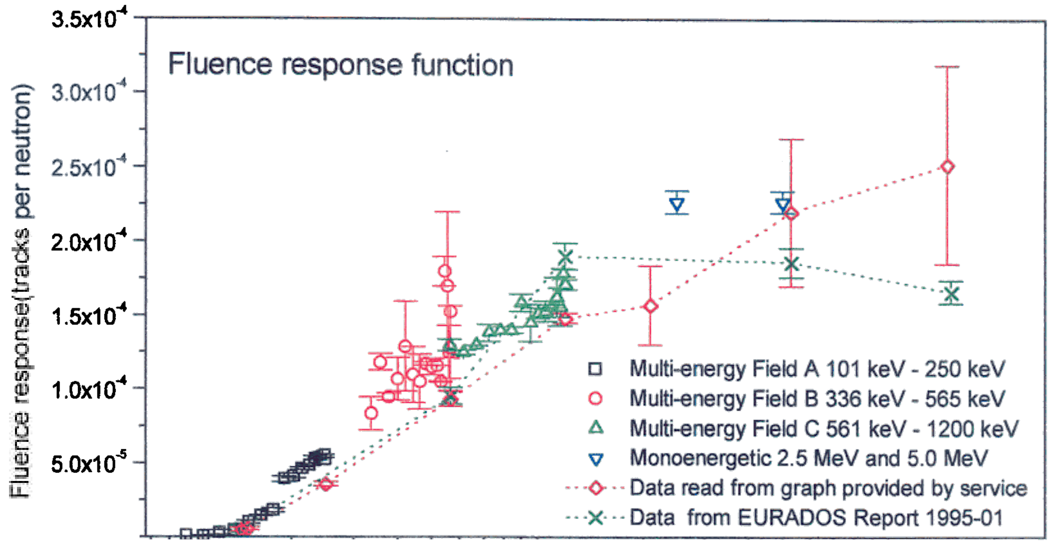

Figure 21. Comparison of present measurements with earlier results for dosemeter set P3

A comparison of the two previous data sets with the present set highlights some of the difficulties of investigating track-etch detector response functions when the characteristics of the systems are sensitive to factors such as changes in the processing techniques or materials, or in the reading. This makes it difficult to know whether differences between measurement sets are due to problems with the measurements or changes in the system. At some energies there is good agreement between the new and the old results, although at others there are differences. Comparing the present data with that supplied by the service shows very reasonable agreement at 150 keV, 1.2 MeV, and 2.5 MeV, although the present measurements are higher at the intermediate energies. For the European intercomparison data there is again reasonable agreement with the present results at 150 keV and 1.2 MeV, although the new measurements are higher elsewhere. The differences are not, however, in general particularly significant when the measurement uncertainties are taken into consideration.

4.3 The NTA film dosemeters

Because only two of the participating dosimetry services offered NTA film dosemeters, it was particularly unfortunate that no results were returned by one of these. The data which were returned, for dosemeter set N1, illustrate the differences between the response functions of PADC based devices and ones based on NTA film. The energy at which fast neutrons begin to be detected is much higher for film, with a response threshold at about 500 to 600 keV. Also, for film, the response continues to increase with energy up to 5 MeV and above. This may give NTA film dosemeters advantages in high-energy neutron fields.

Some earlier response function data, extending from 675 keV to 14.9 MeV were made available by the service operating dosemeter set N1, and these are compared with the present results in Figure 22. Although there is excellent agreement at 5 MeV, below this energy the present measurements are significantly lower than the earlier ones. This difference may well be a genuine change in the response function. Over the course of time changes may have occurred due, for example, to changes in processing techniques and materials. The reading of these dosemeters, which is done manually, depends somewhat on the person reading the film, and this also introduces the possibility of changes as different individuals take on the role of reading the films.

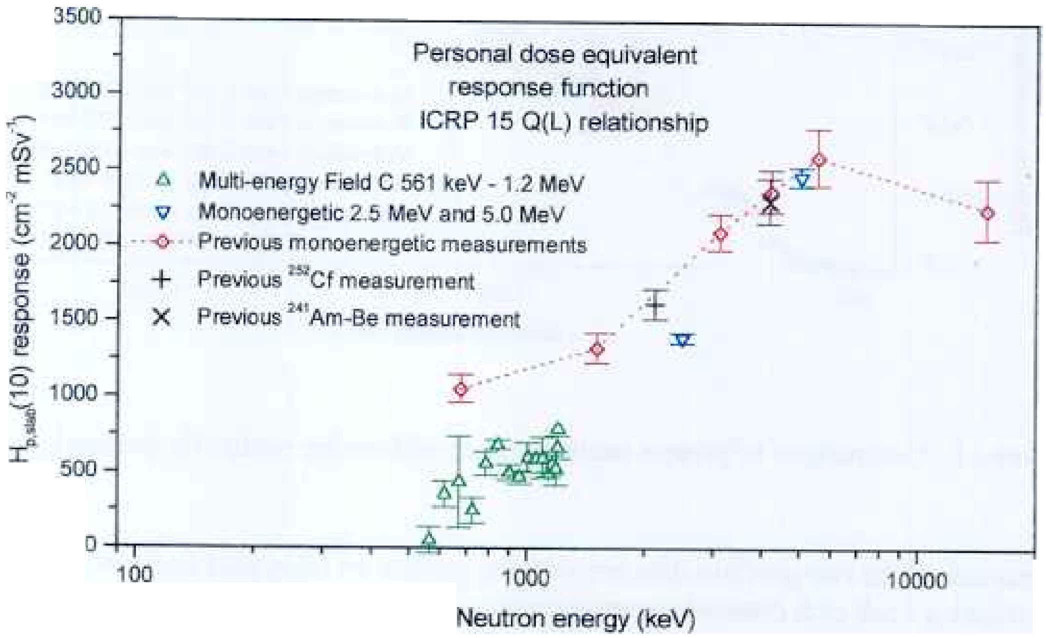

Figure 22. Comparison of present responses with previous measurements for dosemeter set N1

The multi-energy Fields A, B, and C, although very well suited for investigating PADC response functions, cover an energy range which is really too low for NTA film. Although Field C provides useful information about exactly where the response falls to zero, further monoenergetic measurements at higher energies are necessary to provide an adequate characterisation of the shape of the response function over the neutron energy region where the response is greatest.

4.4 Personal dose equivalent response functions for the ICRP 60 Q(L) relationship

In 1991 the ICRP, in Publication 60[(15)], recommended various changes in radiation protection practice, including a reduction of the dose limits, and changes to the dosimetric quantities. The recommendations replace effective dose equivalent as the limiting quantity with effective dose, which is similar in concept, in being a weighted average of organ doses in a body, but is somewhat differently defined. The operational quantities used to estimate the limiting quantity also change because a new Q(L) relationship is recommended for use when calculating the relevant fluence to dose equivalent conversion coefficients. Revised conversion coefficients have been calculated by a number of workers, and an evaluated set of data based on these values has been published[(18)].

The new recommendations of the ICRP have not yet been incorporated into UK legislation. However, the European Commission, in 1996, adopted a revised Basic Safety Standards (BSS) Directive, incorporating the recommendations of ICRP 60. The new BSS must be implemented by member states, and the Directive allows four years for this to happen. New Ionising Radiation Regulations are presently being formulated in the UK (a draft version for comments is already available) which include the ICRP 60 recommendations. Since these new regulations are scheduled to come into force at the start of the year 2000, it is interesting to look at their implications for personal dosemeters response functions.

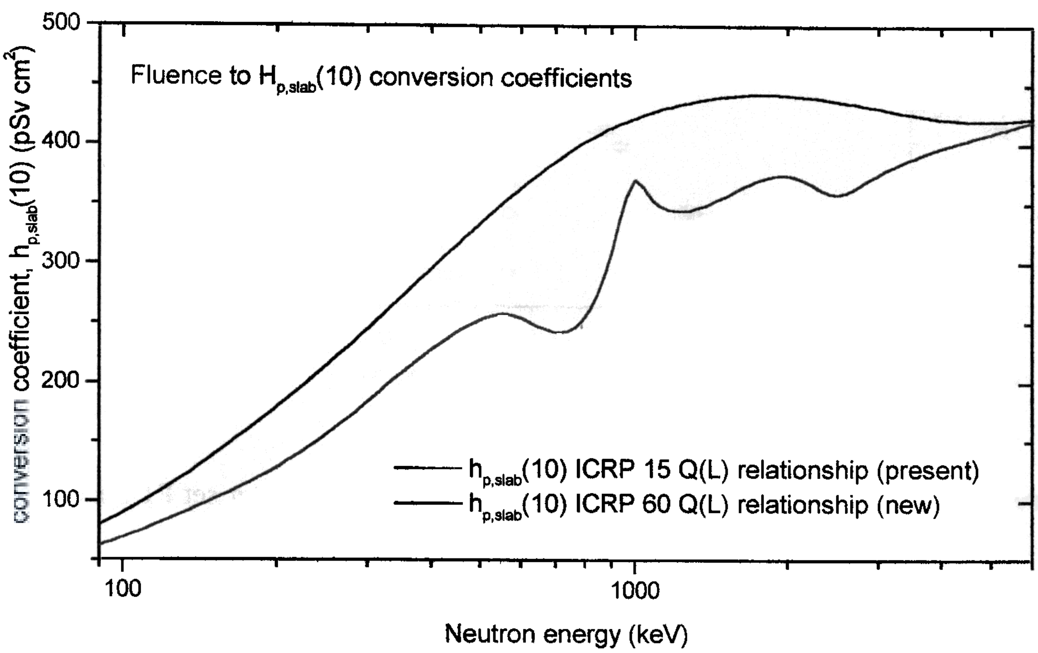

Figure 23. Variation of conversion coefficients, $h_{p,slab}(10)$, between 90 keV and 6 MeV

Figure 23 shows the fluence to dose equivalent conversion coefficients for both the old, i.e. pre-ICRP 60, and the newly recommended Q(L) relationships over the energy range from 90 keV to 1.2 MeV covered by the present response function measurements. The new coefficients are larger than the old values, resulting in a larger value for the personal dose equivalent per unit fluence, and the difference between the old and the new coefficients is greatest near the middle of the range. The response functions for the new quantities will have a different overall magnitude, with fewer tracks per unit personal dose equivalent, and the shape of the response curves will change slightly.

Figures 24, 25, 26, 27 and 28 show the response functions for the dosemeter sets P1, P2, P3, P4 and N1 respectively as derived with the new conversion coefficients.

Some features of the new response functions are common to all the dosemeters. The new conversion coefficients have a smoother variation with neutron energy, and the resulting response functions are also smother, particularly in the region just above 1.0 MeV. The structure in the old conversion coefficients appears not to be reflected by corresponding structure in the dosemeter

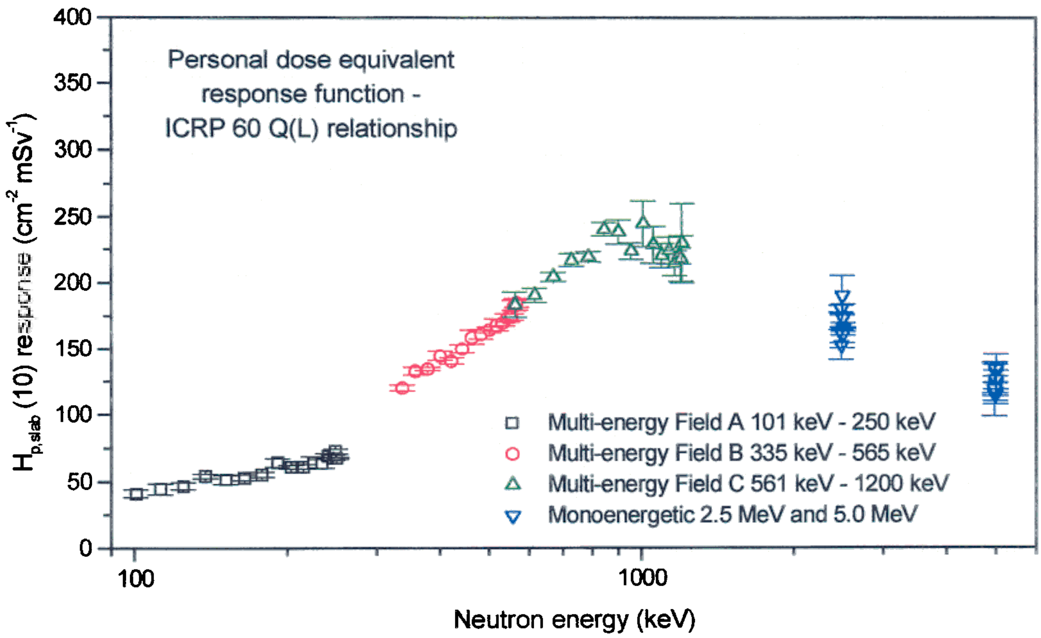

Figure 24. Personal dose equivalent response function for dosemeter set P1 for ICRP 60 Q(L)

track density measurements. If they were, the two would tend to cancel out, and the response functions with the old conversion coefficients would be the smoother.

Peaks and dips in the conversion coefficients are not unrealistic, and can occur because of structure in the cross sections of the ICRU tissue, which in turn give rise to genuine fluctuations in the calculated dose equivalent deposition at 10 mm in the slab phantom. Any such structure must be due to features in the carbon, oxygen, or nitrogen cross sections, rather than the hydrogen cross section which is smooth over the relevant energy range. Since the neutrons giving rise to events in a dosemeter sensor element have only travelled through of the order of 2 mm of material, the effects of any cross section structure in this material tend not to show up, simply because there is so little attenuation. Thus, even if there were genuine fluctuations in the fluence to personal dose equivalent coefficients, one would not normally expect these to be reflected in events in the dosemeters.

The changes in the response function shapes brought about by the use of the new conversion coefficients are not particularly dramatic. In some cases, dosemeter set P1 being an example, the personal dose equivalent response function is somewhat flatter for the new quantity thus improving the dosemeter performance. The change is, however, relatively small. Dosemeters which measure personal dose equivalent satisfactorily for the present quantity will, after re-calibration, in most cases still measure personal dose equivalent satisfactorily for the new quantity. Similarly, dosemeters which are poor for the old quantity will, in all probability, continue to be poor for the new quantity.

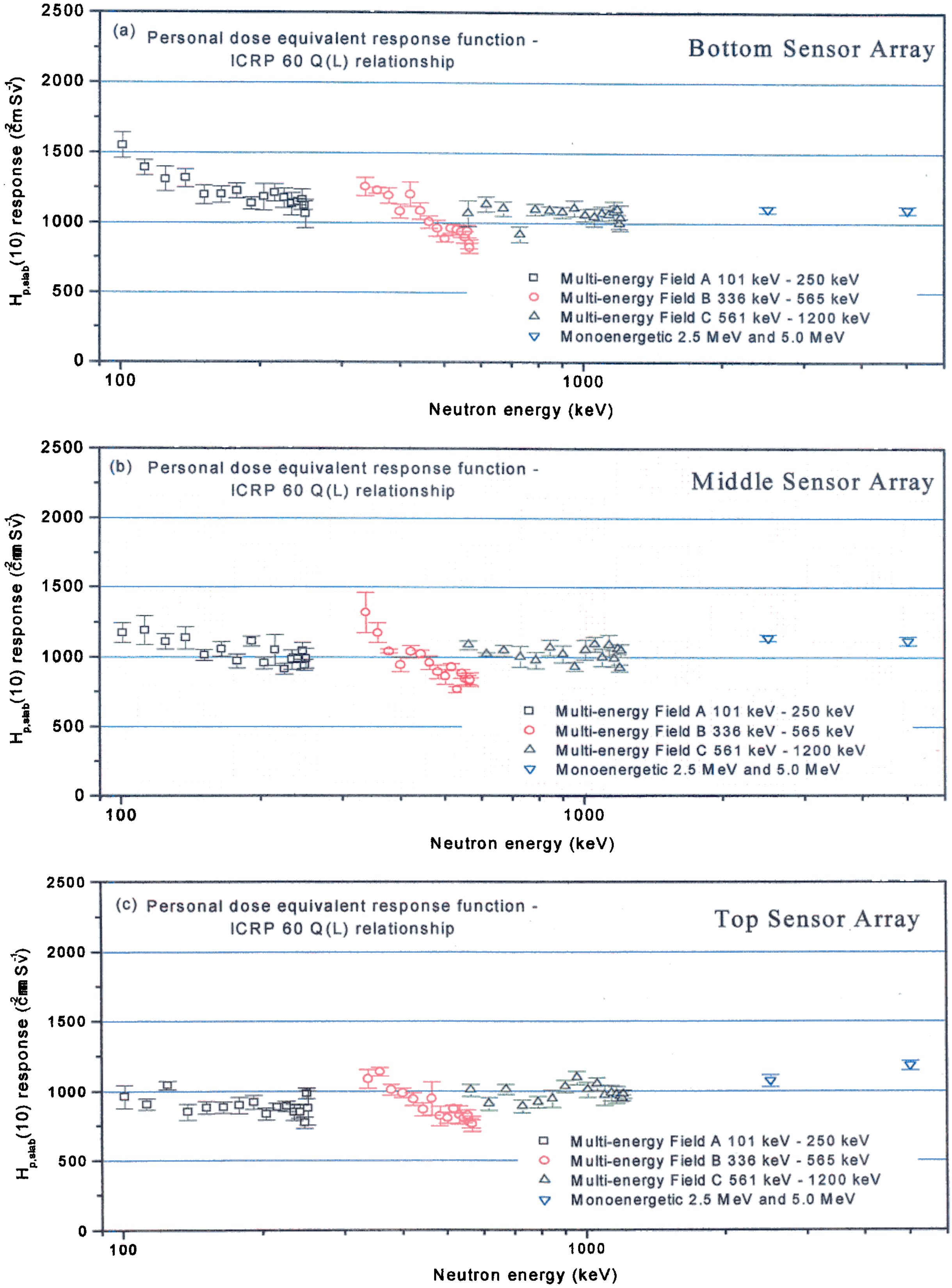

Figure 25. Personal dose equivalent response function for dosemeter set P2 for ICRP 60 Q(L)

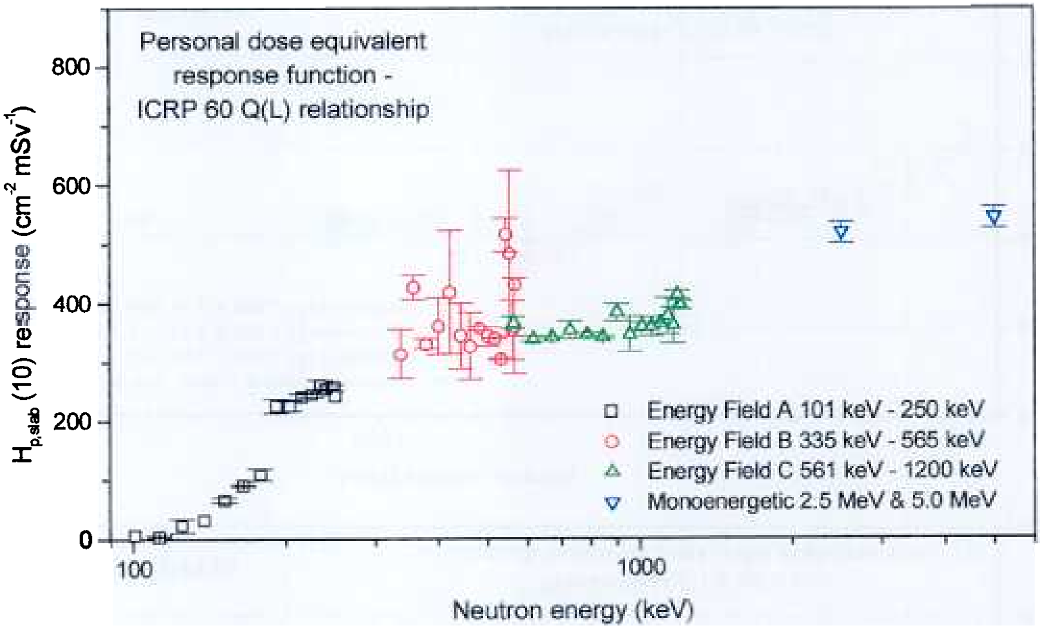

Figure 26. Personal dose equivalent response function for dosemeter set P3 for ICRP 60 Q(L)

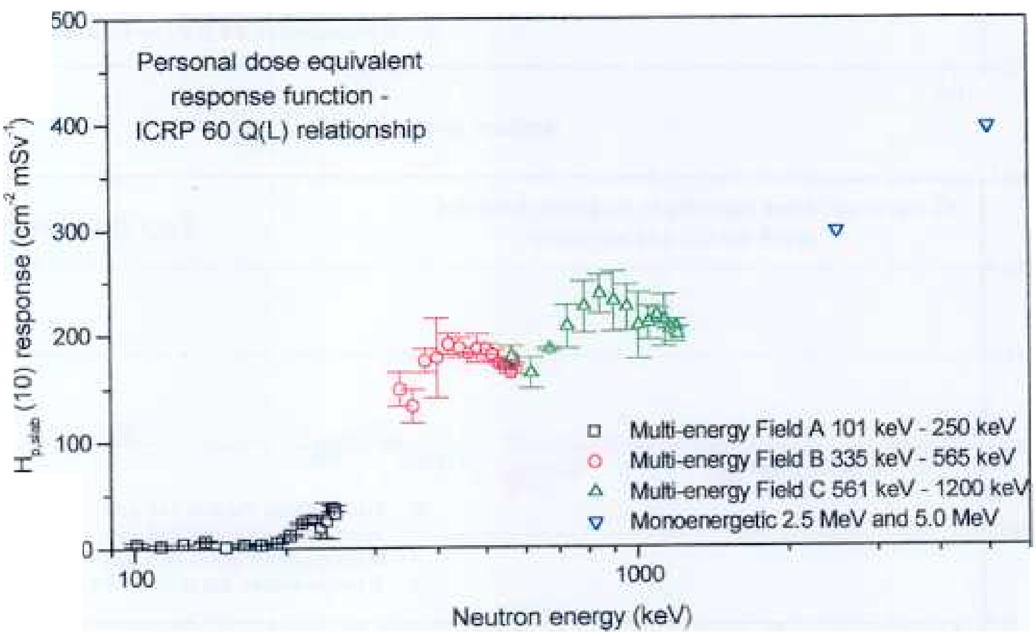

Figure 27. Personal dose equivalent response function for dosemeter set P4 for ICRP 60 Q(L)

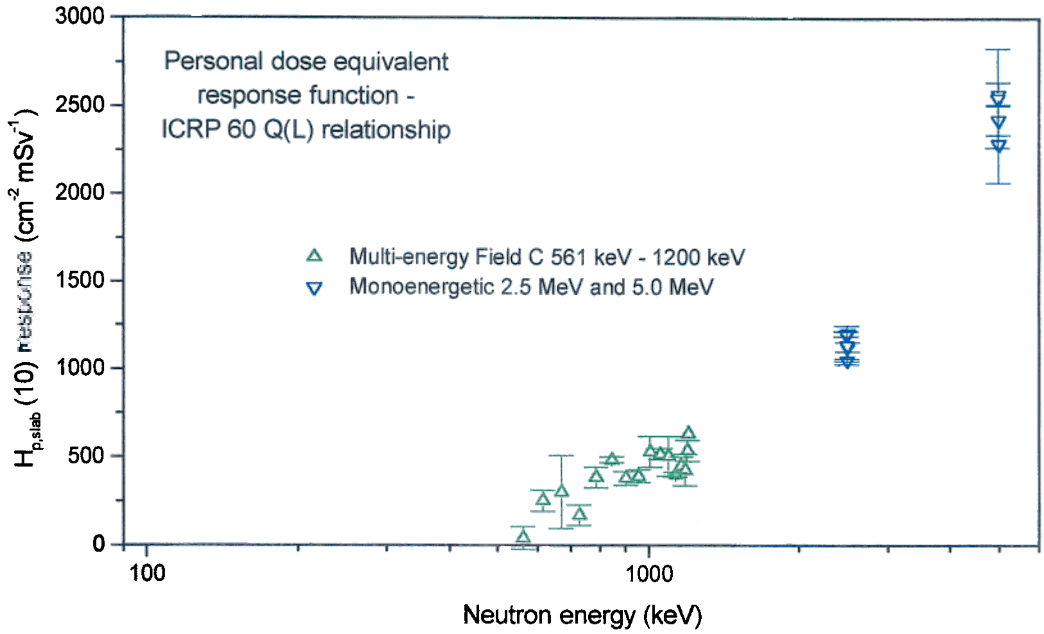

Figure 28. Personal dose equivalent response function for dosemeter set N1 for ICRP 60 Q(L)

5. CONCLUSIONS

The present measurements have provided a good set of response function data for the PADC track-etch and NTA film personal dosemeters currently in use for neutron dosimetry in the UK. There remain several unexplained odd results, in particular, for dosemeter set P2 over the neutron energy range from 336 to 565 keV, and between 336 keV and 1.2 MeV for set P4. A repeat of these measurements, to investigate whether the results are reproducible, would by very desirable. One parameter which might have a bearing on the results is the overall dose equivalent values delivered to the dosemeters. This could be varied to check that the same results are obtained for different integrated dose equivalents.

Dosemeter response functions tend to change with time for a number of reasons. These include: changes to the characteristics of the sensor material, even when always obtained from the same supplier, changes to etching techniques for PADC plastic, and to methods of reading the tracks for both types of sensor elements. This variation highlights the importance of being able to make response function determinations, with sufficient detail, in an efficient manner, without involving prohibitive costs.

The uncertainties shown for the present measurements in the various plots are values of the standard uncertainties (67% confidence level) estimated from the measured spread of the reported readings only. This contribution, labelled here as component (a), is only one of several component uncertainties. For the multi-energy fields additional components arise for: (b) the uncertainty in the measured 0° fluence, (c) the derivation of the fluence at the various angles from that measured at 0°, (d) the effects of room scatter, (e) the lack of a phantom to provide backscatter, and (f) the effects of scattering within the neutron-producing target which introduces a contaminant, nonmonoenergetic, component into the field. For the measurements at 2.5 and 5.0 MeV only effects (a), (b), (d), and (f) are relevant. Typical values for the various uncertainty components are given below.

(a) Values for the standard uncertainty in the reading of a single dosemeter, as derived from the measured spread of the data, appear to be in the range 10 to 15%. (For irradiations to dose equivalent levels near the optimum, this is larger than would be expected if the uncertainty was solely due to Poisson statistics.) Increasing the number of dosemeters irradiated at a particular energy decreases the uncertainty due to the statistical spread, in theory by the square root of the number of measurements. There are some cases, in particular where the uncertainty has been derived from the spread of only two readings, where the standard uncertainty measured was much larger than 15%. In most cases this was due to a single 'rogue' datum, for example one sensor with an anomalously high background.

(b) The uncertainty in the measurement of the neutron fluence at 0° is typically about 4%.

(c) The factors used to derive the fluence at any angle from that at 0° have an uncertainty of about 1%[(12)].

(d) Although no correction is made for the effects of room scatter when dosemeters of these types are irradiated at 75 cm from the source of neutrons, an uncertainty component of 1% is included to allow for the uncertainty in the estimate that the response to these scattered neutrons is negligible.

(e) As noted in Section 2.3, the response of PADC track-etch and NTA film dosemeters to phantom backscatter for neutrons from ^{241}Am-Be and ^{252}Cf sources is about 5%. For lower energies, such as those provided by the multi-energy facilities, the backscatter response is expected to be lower, except perhaps at the very lowest energies for dosemeters with a response to albedo neutrons. A reasonable approach to dealing with backscatter would thus be to add 3% to the multi-energy field results while adding a component of 3% to the uncertainty. This is the best option for anyone wanting the very best estimate of the response function but if the correction is not applied a component of about 5% should be added to the uncertainty.

(f) The uncertainty introduced by target scatter was estimated in section 4.1 to be about 3%.

A full uncertainty analysis for all the data points is rather complex. For example, the uncertainty in the 0° neutron fluence is common for all data measured within a particular multi-energy field. Covariance terms thus exist between these data, and should be taken into account. For the response characteristic measured using the multi-energy fields, the uncertainty, assuming no correction is applied for the missing phantom backscatter, is typically 7% plus the statistical uncertainty for the multi-energy field measurements, and 5% plus the statistical uncertainty for the measurements on-phantom.

Several points of general interest emerge from this work, and these are listed below.

1. Response functions for dosemeters using PADC track-etch plastic do not all exhibit the same shape. This is due to differences in the characteristics of the plastic, the processing, and the

reading. No single response function representative of PADC as a sensor element can therefore be derived.

2. The belief that dosemeters such as those studied here have a sharp threshold below which the response is negligible, and above which the response is proportional to personal dose equivalent, is somewhat of an oversimplification.

3. For dosemeter set P1, and P2 in particular, there is a need to extend the measurements to lower neutron energies. There is also a need to have information on the response function above 5 MeV. This represents somewhat of a problem. With the Van de Graaff accelerator at NPL it is not possible to produce fluence standards between 6 MeV and about 15 MeV. However, with the exception of areas around high-energy accelerators, and at altitudes where cosmic-ray doses become significant, very few neutron fields in which individuals are exposed have a significant dose equivalent component above about 5 MeV. Some data above this energy are, nevertheless, needed. However, in view of the fact that the highest accuracy is not needed, a single measurement at about 15 MeV is usually adequate to extend the data to the region above 5 MeV.

Acknowledgements.

This work was funded by the UK National Measurement System Policy Unit and was part of Deliverable (iv) of Project 3.1 in its 1995 to 1998 Programme for Ionising Radiation Monitoring Metrology. The title of the project was: *An Facility for Determining the Energy Threshold and Near-threshold Response for Neutron Dosimetry.* We would particularly like to thank all the dosimetry services for providing the dosemeters. These were: Defence Radiological Protection Services (DRPS - DERA), the National Radiological Protection Board (NRPB), Integrated Radiological Services Ltd (IRS), and Landauer Inc. At NPL we would like to thank, Graeme Taylor for the target scatter calculations, Martin Burke, and Nicola Horwood for help with the irradiations, and John Winnington and Andrew Bennett for their efficient operation of the Van de Graaff accelerator.

(14) International Commission on Radiological Protection, *Recommendations of the International Commission on Radiological Protection, Protection against Ionizing Radiation from External Sources,* ICRP Publication 15 (Pergamon Press, Oxford) 1970.

(15) International Commission on Radiological Protection, *1990 Recommendations of the International Commission on Radiological Protection,* ICRP Publication 60 (Pergamon Press, Oxford) 1991.

(16) Guldbakke, S. and Schlegel, D., *The Spectral Neutron Fluence Produced by the Interaction of Charged Particles with Solid State Targets (E_n > 1 MeV)*, pp 286-289, Proceedings of the 5th International Conference on Applications of Nuclear Techniques "Neutrons in Research and Industry", Crete, Greece, 9-15 June, edited by George Vourvopoulos, SPIE proceedings series, Volume 2867, 1997.

(17) Schraube, H., Alberts, W.G., and Weeks, A.R., *Fast and High-Energy Neutron detection with Nuclear Track Detectors: Results of the European Joint Experiments 1992/93,* EURADOS Report 1995-01, GSF-Bericht 15/95, GSF-Forschungszentrum, 1997.

(18) International Commission on Radiological Protection, *Conversion Coefficients for use in Radiological Protection against External Radiation*, ICRP Publication 74 (Pergamon Press, Oxford) 1997.